Erasmus University Rotterdam
Erasmus School of Economics

Master Thesis Econometrics and Management Science

# Investment Risk in Global Commodity Markets: Exposure to Climate Policy Uncertainty

Nick Koster (435703)

Supervisor: dr. W. Wang
Second assessor: dr. M.D. Zaharieva

Date final version:
May 1, 2021

**Abstract**

This paper investigates the effect of shocks in global climate policy uncertainty (CPU) on the prices of commodities. In the spirit of Baker et al. (2016), we construct country-level CPU indexes based on newspaper coverage frequency, from which we extract a global factor. We specify a nonlinear autoregressive distributed lag (NARDL) model that incorporates asymmetric dependencies both in the long-run equilibrium relation and short-run dynamics, estimated using a recently advanced two-step procedure. We apply our methodology to monthly prices of futures contracts on six primary commodities over the period 1996-2020. We find evidence of a stable, long-run relationship between each of the price series, global CPU, and a set of macroeconomic control variables. Furthermore, heterogeneous price responses to changes in uncertainty are observed across the commodities, as well as asymmetries in the short-term and longer term. A forecasting exercise reveals that our approach generates more accurate price predictions than important benchmark models in the medium to long term. Moreover, we demonstrate the statistical value of the novel NARDL estimation approach. The results highlight the relevance of climate-related regulatory uncertainty as a source of risk in commodity markets and suggest that investors may hedge their overall position through strategic commodity allocation.

# Contents

# 1 Introduction

Climate change is one of the most pressing issues of this century, affecting people, economies, and the environment around the world. Moreover, its effects are becoming increasingly apparent. Recent reports from the Intergovernmental Panel of Climate Change (IPCC) highlight the danger of human-induced climate change, stressing that the world will face catastrophic consequences unless global greenhouse gas (GHG) emissions are eliminated within the next thirty years (IPCC, 2018). Albeit to varying extents, the developments in each economic sector have been and will continue to be influenced by climate change. From an investment perspective, this has important implications. For instance, physical threats such as floods or droughts may directly impact assets or distribution chains, whereas climate-related regulatory changes could have profound repercussions for entire industries. Of all asset classes, commodities are most directly affected by climate change and its associated uncertainties, and commodity allocations may thus be hurt by unintended exposure to this underlying risk factor. For investors and financial institutions participating in commodity markets, identification of such a factor and estimation of its dynamic relationship with commodity prices is therefore essential. Consequently, thorough knowledge regarding both components is required to manage the financial risks from climate change and potentially exploit differences across commodities.

Following the seminal work of Sharpe (1964) and Lintner (1965), that introduces the capital asset pricing model, a long string of literature has emerged that relates the prices and returns of financial assets to systemic risk factors. The ongoing search for relevant risk factors has resulted in a broad range of proposed measures. In this regard, macroeconomic variables have attracted particular attention. Generally, such variables are deemed to represent market-wide forces, thereby constituting sources of investment risk (Chen et al., 1986). While traditionally primarily confined to studies on real economic activity, partly due to the global financial crisis of 2008 uncertainty measures have gained more prominence in asset valuation. For example, Pástor and Veronesi (2012) and Brogaard and Detzel (2015) employ the index of economic policy uncertainty (EPU) of Baker et al. (2016) to help explain cross-sectional variation in stock prices. More recently, several studies have researched the links between commodity markets and various measures of uncertainty. Specifically, Tan and Ma (2017) investigate the price response of primary commodities to changes in uncertainty using a measure of macroeconomic uncertainty, whereas Bilgin et al. (2018) also adopt the EPU index to examine the same relation. Overall, these studies provide ample evidence of the pertinence of uncertainty in financial markets.

With respect to climate change, uncertainty stems from multiple sources, such as the possibility of extreme weather events or potential sudden changes in regulations, technology, and consumer tastes (Engle et al., 2020). The economic implications for commodities of these uncertainties and the respective risks have previously been analyzed by a number of studies. For instance, Reilly et al. (1994) adopt a policy simulation approach to assess changes in the spot prices of agricultural commodities under different climate scenarios, reflecting uncertainty concerning climate developments and adaptation strategies. Here, they illustrate considerable heterogeneity in the price responses across scenarios. Furthermore, Brunner (2002) finds a significant impact of the El

Niño–Southern Oscillation—which is a recurring climate pattern whose dynamics are substantially altered by climate change—on the prices of non-oil primary commodities. In a more recent study, Diffenbaugh et al. (2012) evaluate the sensitivity of corn price volatility to changes in climate volatility, emphasizing particular sensitivity in the presence of a biofuels mandate. Yet, examinations of the link between commodities and uncertainty surrounding climate-oriented actions of governments, who have a crucial role in tackling climate change, are limited. Moreover, the existing studies mainly focus on isolated events or employ scenario-based approaches. As such, they do not account for market-wide risk factors underlying commodity markets.

In this paper, we investigate the dynamic relationship between the prices of primary commodities and global climate policy uncertainty (CPU), related to government responses to climate change. In the context of commodities, as indicated by Engle et al. (2020), potential climate-related policy measures are especially relevant to investors. Namely, in order to address climate change we should focus on mitigation—that is, reducing greenhouse gas emissions—and adaptation, meaning to prepare for unavoidable consequences (IPCC, 2014). Both of these require decisive political action and are strongly connected with commodity markets. On the one hand, primary commodities like energy and industrial commodities have significant GHG footprints. For these commodities, environmental policies such as the Clean Power Plan proposed by the Obama administration in 2015 or carbon taxation schemes may cause negative demand shocks. In fact, climate policy actions could render entire fossil fuel reserves redundant, leading to so-called stranded assets (Caldecott et al., 2016). On the other hand, commodities are highly dependent on the success of adaptation efforts, particularly agricultural products. For instance, adaptation policies can help make crops more resilient to climate change, preventing negative supply shocks in case of extreme weather events. This way, regulatory responses to climate change pose both risks and opportunities for practitioners.

The fundamental task that arises with uncertainty-based analyses is that of determining an appropriate measure of uncertainty. Regarding climate policy uncertainty, a few approaches have been suggested in the literature. Most notably, Fuss et al. (2008) and Yang et al. (2008), among others, consider a real options framework, in which uncertainty is modeled in terms of the evolution of $CO_2$ prices. Simulating carbon price shocks or possible price paths, a recursive optimization procedure is then used to evaluate investment opportunities in the electric power sector. Alternatively, Fried et al. (2021) aim to assess the macroeconomic impact of climate policy uncertainty in the U.S. by studying how the probability that a carbon tax will be introduced affects the investment decisions of entrepreneurs, using a general equilibrium model. However, the present methods depend greatly on the assumptions about the underlying stochastic processes. Additionally, they focus on the influence of the uncertain arrival of a single carbon-related policy on the behavior of private investors, thereby hampering analysis over time or comparison across commodity classes, sectors, or countries.

Instead, inspired by Baker et al. (2016), we propose to construct a climate policy uncertainty index based on newspaper coverage frequency. By means of content analysis of newspaper articles, Baker et al. (2016) create country-level EPU indexes that reflect both short-term and longer term concerns, related to uncertainty about the implementation of economic policies and the economic ramifications of policy actions. This time-varying

measure of uncertainty has become widely used by researchers and practitioners, in part because it enables continuous monitoring of policy risk and allows for extension to specific types of EPU. For example, Baker et al. (2016) develop indexes of trade policy uncertainty and health care policy uncertainty, among others. In a similar fashion, we augment the array of category-specific EPU indexes with a novel index capturing (economic) uncertainty regarding the adoption and details of climate change policies. A key advantage of this approach over current practices is that it encompasses multiple dimensions of regulatory uncertainty, in line with our aim of establishing a market-wide risk factor. Moreover, we can use the approach to obtain CPU indexes for a range of countries, from which global uncertainty can be extracted using a multi-level factor model, similar to Kose et al. (2003). Lastly, the resulting uncertainty factors are directly associated with climate-related political developments and can be straightforwardly incorporated in a regression framework.

To describe the relationship between commodity prices and climate policy uncertainty, we specify a dynamic linear regression model that allows us to trace the evolution of prices in response to a shock in uncertainty. Specifically, our analysis is performed within an autoregressive distributed lag (ARDL) framework (Pesaran, 1997; Pesaran and Shin, 1995). In this framework, long-run equilibrium relations and short-run dynamics are modeled simultaneously, consistent with recommendations from related studies. For instance, using an ARDL model, He et al. (2010) establish that changes in global economic activity affect the price of crude oil through both long-run equilibrium conditions and short-run dependencies. Similarly, based on a panel cointegration test, Nazlioglu and Soytas (2012) find a long-run relationship among the price of oil, prices of agricultural commodities, and the real effective U.S. dollar exchange rate. Compared to alternative methods capable of dealing with non-stationary time series, which empirical evidence usually suggests commodity prices and most macroeconomic variables are, the ARDL approach has important benefits. In particular, we can test for the existence of a cointegrating relation irrespective of whether the exogenous variables are purely $I(0)$, purely $I(1)$, or a mixture of both (Pesaran et al., 2001). Contrarily, conventional cointegration techniques used when employing error correction models (ECMs) require all variables to be integrated of order one, which entails pre-testing and thereby introduces additional uncertainty into the analysis. Another approach presented in the literature is to simply transform non-stationary variables to stationary ones, e.g., through first differencing, such that models like (structural) vector autoregressions are applicable. Nevertheless, as noted by Engle and Granger (1987), this may disregard valuable long-run information often contained in economic time series.

We extend the model to account for asymmetry in the commodity price responses to positive and negative changes in policy uncertainty. Namely, literature provides convincing evidence that the symmetry assumed in the ARDL model may be too restrictive. Generally, the impact of positive uncertainty shocks on economic or financial outcomes tends to be greater than that of negative shocks (Grier et al., 2004; You et al., 2017). Shin et al. (2014) demonstrate that such asymmetries can be readily incorporated in the ARDL model by means of partial sum decompositions of the exogenous variable(s) of interest, highlighting another key feature of the ARDL-based approach. The resulting nonlinear ARDL (NARDL) model accommodates all combinations of long-run and short-run (a)symmetry. Moreover, it encompasses numerous regime-switching models like the

smooth transition or Markov-switching ECM, in which asymmetries are generally limited to the error correction mechanism. Furthermore, the NARDL framework jointly models cointegration and asymmetric dependencies. While the NARDL model is estimable in a single step by ordinary least squares (OLS), Cho et al. (2020) have recently stressed that the model exhibits an asymptotic singularity issue associated with perfectly collinear time trends in the partial sum processes. They derive a two-step estimation procedure in which the long-run relationship and short-run dynamics are estimated separately, that is both analytically tractable and robust to serial correlation and endogeneity. Accordingly, besides the single-step approach, in this study we adopt the two-step estimation approach of Cho et al. (2020) and assess its statistical implications.

The purpose of this paper is twofold: (1) to examine global climate-related regulatory uncertainty as a source of risk underlying commodity prices and capture their dynamic relation, and (2) to establish whether adopting the two-step NARDL estimation procedure of Cho et al. (2020) can enhance statistical inference. Thereby, we aim to contribute to two streams of literature. First, in the spirit of Baker et al. (2016), we add to the existing work on asset pricing by developing a novel risk factor for commodities. Second, consulting recent advances in ARDL modeling, we present the first empirical application of the NARDL estimation procedure of Cho et al. (2020) and demonstrate its validity in a setting with both symmetric and asymmetric regressors.

We apply our methodology to monthly prices of futures contracts on six primary commodities over the period 1996-2020. In a first stage, we establish the presence of cointegration between each of the price series, the global level of CPU, and a set of macroeconomic and financial control variables. Following this, we estimate the corresponding long-run relationships and demonstrate asymmetry in the price responses to positive and negative changes in uncertainty, as well as heterogeneity in the responses across commodities. For example, in line with our expectations, we find a strong negative long-run association between CPU and the prices of oil and gas. For gold this relation is positive, consistent with the notion of gold as a safe haven in times of market turmoil. Moreover, the response of these commodities to positive uncertainty shocks is stronger than to negative shocks. Next, we examine the error correction mechanisms and short-run dynamics. The results indicate that it takes around 4 to 6 months for the commodity prices to correct 50% of any deviation of global CPU from the long-run equilibrium. Here, the exact patterns of dynamic price adjustment are highly depend on the commodity. Evaluating the economic value of our methodology by means of a forecasting exercise, we conclude that the two-step NARDL approach outperforms important benchmark models in the medium to long term based on forecast accuracy. The two-step approach also performs better than the traditional one-step approach, which is likely due to the fact that the former yields more precise parameter estimates. For participants in commodity markets, the findings emphasize the relevance of identification of the systemic uncertainty factor, as well as knowledge regarding the exposure of individual commodities to this factor. While political developments need to be closely monitored, investors may limit the overall exposure of their position to changes in CPU through strategic commodity allocation, that is, beta hedging.

The remainder of this paper is organized as follows. Section 2 introduces the data and elaborates on the construction of the climate policy uncertainty index. Section 3 outlines the dynamic asset pricing framework

and the proposed estimation approach. Section 4 presents and discusses the results of our empirical study. Section 5 summarizes and concludes our research. Lastly, Section 6 provides a discussion of the paper.

# 2 Data

In this section, we discuss the uncertainty index, price data, and macroeconomic variables used in our research. Section 2.1 introduces the measure of climate policy uncertainty and presents both the country-level indexes and the global index. In Section 2.2 and 2.3, we give an overview of the considered commodities and macroeconomic control variables, respectively. Lastly, we examine stationarity of the stochastic processes in Section 2.4.

## 2.1 Climate Policy Uncertainty Index

### 2.1.1 Country-Level Indexes

We construct an index of climate policy uncertainty (CPU) that reflects the level of regulatory uncertainty regarding the adoption and details of climate change policies. For this purpose, we follow the approach of Baker et al. (2016), who aim to enhance the understanding of economic and political developments through content analysis of newspaper articles. Specifically, they create country-level indexes of economic policy uncertainty (EPU) based on newspaper coverage frequency, utilizing online newspaper databases to search for articles that contain at least one term in all three EPU categories: the economy, policy, and uncertainty. These indexes should capture both short-term and longer term concerns, related to uncertainty about when and which economic policies will be implemented, as well as the economic effects of policy actions. The main premise of this approach is that newspaper articles reflect public interest and concern regarding particular topics. At the same time, coverage of scientific subjects by the mass media may influence public perception and action, for example stressed by Boykoff and Rajan (2007) in the context of climate change.

As emphasized by Baker et al. (2016), their approach has various desirable features. For instance, it is readily extended to many countries, allows for analyses over sustained periods of time, and enables near real-time updating of the uncertainty indexes. Importantly, the newspaper-based method also offers the flexibility to construct category-specific sub-indexes, such as the index of health care policy uncertainty or the newly created COVID-induced uncertainty index (Baker et al., 2016, 2020). Given the aim of our research, the EPU index thus provides a useful starting point. Similar to the category-specific EPU indexes developed by Baker et al. (2016), we focus on the subset of EPU articles that also contain terms related to the climate or climate change. This way, we arrive at the proposed measure of climate policy uncertainty used in our study.

We perform our research in an international setting and are therefore interested in the level of global climate policy uncertainty. To derive global CPU levels, we first construct monthly indexes for the United States, United Kingdom, Australia, and China, using newspaper data obtained from the Factiva global news database. We consider these four particular countries, as they are all members of the G20 with English-

language newspapers for which the Factiva database offers historical newspaper articles over an extended period of time. For each country we consider articles in multiple leading newspapers, published between July 1996 and October 2020. Our start date is equal to the first month for which all but two newspapers are available and the end date is chosen to account for a time lag in the publication of articles. Following the procedure of Baker et al. (2016), in each month we count per newspaper the number of articles that contain one or more terms in the CPU categories: the economy, policy, uncertainty, and the climate. This count is then scaled by the total number of articles published in a particular newspaper in each month. Subsequently, the monthly series of scaled counts are scaled per newspaper to have unit standard deviation from January 2001 to October 2020. Finally, per country we average the standardized scaled counts over the newspapers by month to obtain the CPU indexes for the United States, United Kingdom, Australia, and China.

The exact search terms for the three EPU categories are derived from Baker et al. (2016) and the EPU website.[1] The economy, uncertainty, and policy terms—the last of which are country specific—are selected by Baker et al. (2016) based on an extensive human audit study, such that the sum of false positive and false negative error rates is minimized. Moreover, they demonstrate that the EPU indexes are closely related to other measures of economic uncertainty like the VIX and do not suffer from political slant which could skew newspaper coverage, thereby alleviating concerns regarding reliability, accuracy, and bias of the approach. We augment the collection of search terms with the set of search terms for the climate category that includes "climate," "carbon," "emissions," and "greenhouse," inspired by the climate change vocabulary of Engle et al. (2020). This vocabulary is based on a broad set of authoritative documents on climate change and indicates the frequency with which each word or phrase appears, allowing us to identify the most relevant terms. For more details on the selection of the climate terms, as well as the full set of search terms and newspapers used in the construction of the CPU indexes, we refer to Appendix A.

Figure 1 plots the standardized CPU indexes for the United States, United Kingdom, Australia, and China over the period July 1996-October 2020. As expected, our CPU indexes are moderately to strongly correlated with the EPU indexes of Baker et al. (2016), with correlation coefficients ranging from 0.54 for the U.S. to 0.66 for China. Looking at the trends in the figure, several similarities across the countries are apparent. In particular, we notice that the levels of uncertainty were relatively low before 2006. After 2006 the four CPU indexes experienced an increase, driven, among others, by new scientific evidence on the dangers of climate change, provided for example by the influential fourth IPCC report published in September 2007 (IPCC, 2007). Moreover, uncertainty grew further due to unsatisfactory political responses to climate change, exemplified by the failure of the participating nations to deliver a climate deal during the Copenhagen Climate Change Conference held in December 2009. In recent years, climate policy uncertainty reached all-time highs for the U.S., U.K., and China. This trend is in line with the growing public awareness of climate change and its the potential catastrophic consequences (see Leiserowitz et al., 2020; Thackeray et al., 2020, e.g.). Overall, Figure 1 provides support for the existence of a common factor underlying the country-level CPU indexes.

[1] See `www.policyuncertainty.com/index.html`.

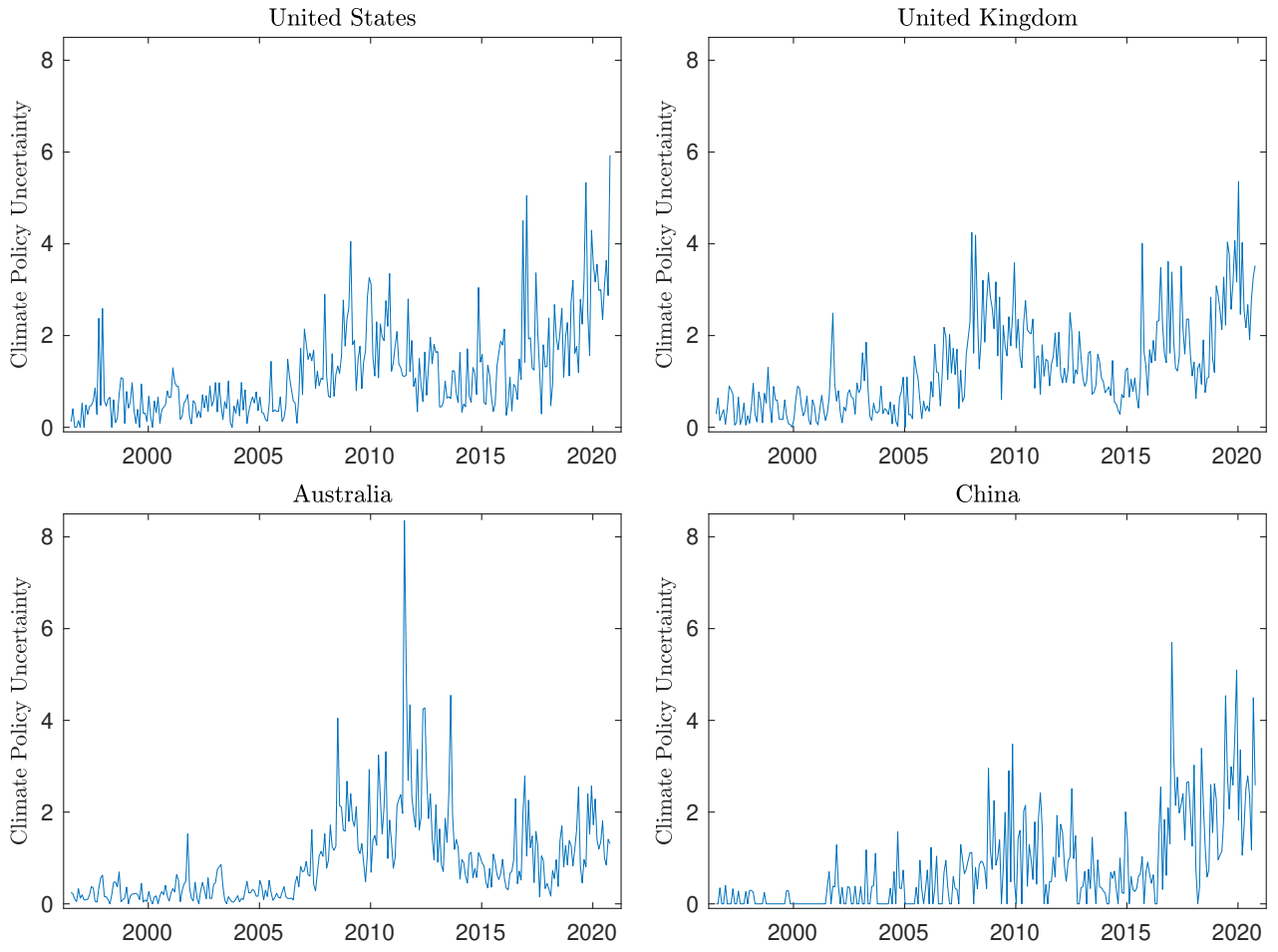


Figure 1: This figure plots the standardized climate policy uncertainty indexes for the United States, United Kingdom, Australia, and China over the period 1996:7-2020:10.

### 2.1.2 Global Index

We intend to extract a global climate policy uncertainty index from the country-level indexes. Namely, we study prices in international commodity markets, which are not necessarily associated with one particular country. Instead, commodity prices tend to be driven by global economic forces (Dwyer et al., 2011; Erten and Ocampo, 2013). Being among the first to distinguish between a national and global component of uncertainty, Berger et al. (2017) emphasize that the latter represents an essential independent factor with key international economic and financial implications. Accordingly, we exploit the observed co-movement of the four CPU indexes presented above, which is assumed to be driven by an underlying global factor. In particular, similar to Kose et al. (2003) and Berger et al. (2017), we specify a dynamic factor model in which the variation in CPU levels for each country is characterized by two dynamic, latent factors: a world factor and a country-specific factor. By imposing a multi-level factor structure, the model offers a clear economic interpretation of the latent factors (Bai and Wang, 2015).

Let $CPU_{i,t}$ denote the climate policy uncertainty index for each country $i \in \{1, \dots, N\}$ and month $t \in \{1, \dots, T\}$, and $f_t^W$ and $f_{i,t}$ the unobserved world and country-specific factor, respectively. Assuming that the factors follow a vector autoregressive process of order $p$, we specify the following dynamic factor model:

$$\begin{bmatrix} CPU_{1,t} \\ \vdots \\ CPU_{N,t} \end{bmatrix} = \begin{bmatrix} \alpha_1 \\ \vdots \\ \alpha_N \end{bmatrix} + \begin{bmatrix} \beta_1 & \gamma_1 & & \\ \vdots & & \ddots & \\ \beta_N & & & \gamma_N \end{bmatrix} \begin{bmatrix} f_t^W \\ f_{1,t} \\ \vdots \\ f_{N,t} \end{bmatrix} + \begin{bmatrix} \eta_{1,t} \\ \vdots \\ \eta_{N,t} \end{bmatrix}, \quad \text{where} \quad \begin{bmatrix} \eta_{1,t} \\ \vdots \\ \eta_{N,t} \end{bmatrix} \sim \mathcal{N}(0, \Sigma_\eta), \tag{1}$$

$$\begin{bmatrix} f_t^W \\ f_{1,t} \\ \vdots \\ f_{N,t} \end{bmatrix} = \Phi_1 \begin{bmatrix} f_{t-1}^W \\ f_{1,t-1} \\ \vdots \\ f_{N,t-1} \end{bmatrix} + \ldots + \Phi_p \begin{bmatrix} f_{t-p}^W \\ f_{1,t-p} \\ \vdots \\ f_{N,t-p} \end{bmatrix} + \begin{bmatrix} \varepsilon_t^W \\ \varepsilon_{1,t} \\ \vdots \\ \varepsilon_{N,t} \end{bmatrix}, \quad \text{where} \quad \begin{bmatrix} \varepsilon_t^W \\ \varepsilon_{1,t} \\ \vdots \\ \varepsilon_{N,t} \end{bmatrix} \sim \mathcal{N}(0, \Sigma_\varepsilon), \tag{2}$$

with $\Phi_1, \dots, \Phi_p$ unrestricted matrices of autoregressive parameters and $\Sigma_\eta$ and $\Sigma_\varepsilon$ diagonal covariance matrices. Of particular interest in this system is $f_t^W$, capturing the level of global climate policy uncertainty. In order to estimate the model specified by Equations (1) and (2), we can write the model in state-space form and use the expectation-maximization (EM) algorithm to obtain smoothed estimates of the latent factors (Dempster et al., 1977). Relative to maximum likelihood, EM tends to get stuck less often in local optima and is better suited for estimation in large parameter spaces. However, as the standard EM algorithm is unable to take parameter restrictions into account, we adjust the algorithm to allow for linear constraints on the parameter matrices. The derivations and details of the estimation procedure can be found in Appendix B.

The smoothed estimates of the global uncertainty factor over the period July 1996-October 2020 are displayed in Figure 2. The graph is annotated with notable CPU-related events that, considering the timing, likely caused the respective spikes. In line with our previous observations, global climate policy uncertainty increased rather strongly from 2006 to 2009 and subsided afterwards, before reaching considerable highs in 2016 and 2020. Furthermore, we find various large shocks in the uncertainty index, both positive and negative, for instance during the period preceding the 2016 United States presidential election. Interestingly, our index agrees with the World Uncertainty Index of Ahir et al. (2018) that uncertainty levels were at an all-time high last year. Lastly, we find a moderate correlation of 0.43 of the global CPU index with the WSJ Climate Change News Index of Engle et al. (2020)—which reflects all long-run risks associated with climate change that are potentially relevant to investors—over the period July 1996-June 2017.

## 2.2 Commodities

Next, we introduce the data set containing the commodity price series under study. The series are obtained from Datastream and correspond to monthly settlement prices of a range of nearest to maturity commodity futures contracts over the period from July 1996 to October 2020. Here, six primary commodities across three broad classes are considered: light crude oil, natural gas, gold, copper, sugar, and wheat. This selection of

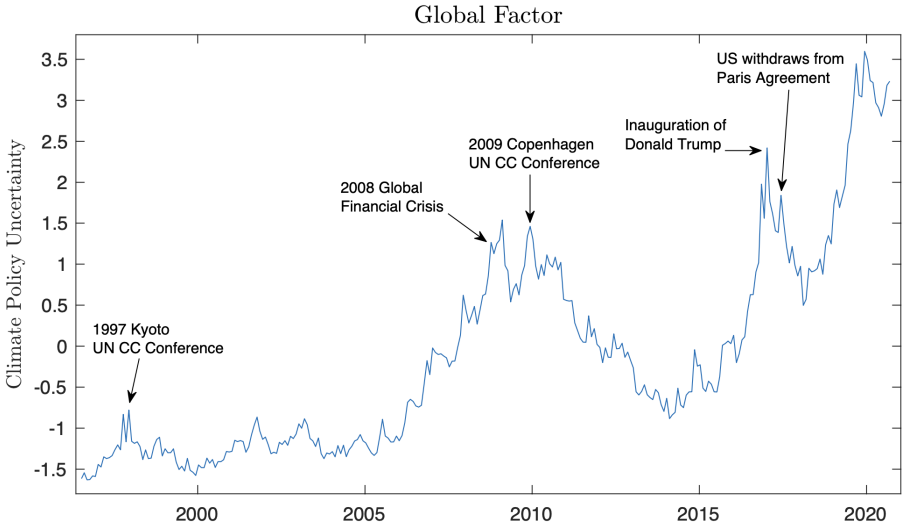


Figure 2: This figure plots the smoothed estimates of the global climate policy uncertainty factor over the period 1996:7-2020:10.

commodities is determined based on relevance with respect to climate policy uncertainty, importance in global markets, and data availability. Furthermore, we focus on nearest-to-maturity contracts because of their high liquidity, which limits market liquidity risk and attracts speculators and investors. The choice of futures instead of spot prices is motivated by three reasons. First, due to their physical nature, commodity spot markets tend to be more limited to or dependent on geographies than futures markets. Second, commodity futures prices converge towards spot prices as the futures contract approaches the delivery month, while commodity investors primarily participate in futures markets (Gorton and Rouwenhorst, 2006).[2] Third, futures markets incorporate new information more quickly than spot markets. For more details regarding the futures contracts, as well as time series plots of the commodity prices, we refer to Appendix C.1.

Given the distinct characteristics of each of the commodities, we expect that the dynamic relationships between the price series and climate policy uncertainty vary considerably across the commodities. Of the set of commodities, the energy commodities have the most evident link with climate-related regulatory uncertainty. For instance, investors may be less drawn towards oil in times of heightened uncertainty regarding carbon taxes. Gold, on the other hand, is traditionally seen as a safe haven, thereby attracting investments in times of market turmoil (Baur and Lucey, 2010). By focusing on this cross-section of the commodity market, we should be able to gain a broad understanding of the impact of climate policy uncertainty on the behavior of financial investors.

## 2.3 Control Variables

Previous literature has identified various key drivers of international commodity prices, including factors related to the traditional forces of supply and demand, as well as financial factors. Accordingly, to isolate the

[2]The use of nearest futures prices as a proxy for spot prices is common in the literature, e.g., see Fama and French (2016).

effect of global climate policy uncertainty on the commodities, in this study we aim to control for the main determinants of commodity prices using a set of five macroeconomic and financial variables.

Specifically, we consider the Kilian index proposed by Kilian (2009) with the recent correction of Kilian (2019), available from the Federal Reserve Bank of Dallas.[3] This index uses cargo shipping rates to construct a measure of global real economic activity in industrial commodity markets, which should capture changes in global aggregate demand for commodities. As demonstrated by Kilian and Zhou (2018), the Kilian index is particularly suitable for modeling commodity markets, relative to alternative measures of global real economic activity such as proxies for global industrial production. Besides, we include the Morgan Stanley Capital International (MSCI) World Index (Coleman, 2012; Drachal, 2016). This index is available from the MSCI website and consists of a wide range of large- and mid-cap companies across developed market countries.[4] Thereby, the index serves as a proxy for the condition of global financial markets.

In addition, we use three control variables obtained from the Federal Reserve Bank of St. Louis.[5] First, as argued by Frankel (2006), among others, (short-term) interest rates positively affect the supply of commodities, thus influencing commodity prices. Moreover, high interest rates increase the cost of carrying commodity inventories—i.e., the cost of carry, which is an important concept in commodity futures markets—thereby reducing the demand for storable commodities. Therefore, we include the 3-month London Interbank Offered Rate (LIBOR), which is a key benchmark in international monetary markets and impacts financial institutions and consumers around the globe (Arango et al., 2011). Second, we consider the nominal effective exchange rate for the United States, computed as a trade-weighted average of bilateral exchange rates. Namely, changes in the U.S. dollar exchange rate tend to influence commodity prices through various channels, such as that of the purchasing power of commodity-exporting countries (Breitenfellner and Cuaresma, 2008; Gilbert, 1989). Lastly, we aim to control for inflation by incorporating the seasonally adjusted U.S. consumer price index (CPI). The time series plots of the control variables are presented in Appendix C.2. In Appendix C.3, we report descriptive statistics of all variables used in the empirical study.

## 2.4 Unit Root Tests

Before we turn to the methodological framework, we assess stationarity of all considered time series. Namely, the appropriateness of any empirical approach is dependent on the exact orders of integration of the variables. For instance, VAR models require that all series are stationary (Sims, 1980). While non-stationary variables can be converted into stationary processes, in the presence of common stochastic trends such an approach would disregard valuable information on long-run relationships between the variables. In order to establish the correct direction for the remainder of this research, it is therefore essential to investigate stationarity (see Shrestha and Bhatta, 2018, e.g.).

[3] See `www.dallasfed.org/research/igrea`.

[4] See `www.msci.com/end-of-day-data-search`.

[5] See `fred.stlouisfed.org`.

Table 1: Unit Root Tests

| | Level | | | | First Difference | | | |
|---|---|---|---|---|---|---|---|---|
| Variable | ADF | PP | KPSS | ZA | ADF | PP | KPSS | ZA |
| ln oil | −1.72 | −1.90 | 0.90*** | −4.58 | −15.09*** | −15.03*** | 0.12 | −11.45*** |
| ln gas | −2.66 | −2.60 | 0.84*** | −5.57*** | −17.53*** | −17.58*** | 0.07 | −12.41*** |
| ln gold | −1.84 | −1.90 | 0.64*** | −3.43 | −20.59*** | −20.46*** | 0.23 | −15.23*** |
| ln copper | −1.52 | −1.81 | 0.73*** | −3.75 | −15.50*** | −15.63*** | 0.09 | −10.28*** |
| ln sugar | −2.50 | −2.64 | 0.51*** | −4.28 | −16.47*** | −16.47*** | 0.06 | −11.35*** |
| ln wheat | −2.90 | −2.72 | 0.58*** | −4.63 | −19.07*** | −19.28*** | 0.10 | −14.13*** |
| CPU | −0.73 | −1.08 | 0.27*** | −2.81 | −20.19*** | −19.99*** | 0.25 | −11.83*** |
| Kilian | −3.35** | −2.86** | 0.98*** | −5.03** | −13.03*** | −12.74*** | 0.04 | −12.09*** |
| ln MSCI | −2.29 | −2.59 | 0.34*** | −3.95 | −15.27*** | −15.28*** | 0.05 | −12.40*** |
| LIBOR | −1.65 | −1.75 | 0.34*** | −3.12 | −12.29*** | −12.71*** | 0.09 | −9.34*** |
| ln FX | −1.95 | −1.65 | 0.74*** | −4.11 | −11.09*** | −10.86*** | 0.15 | −11.28*** |
| ln CPI | −1.20 | −1.24 | 1.05*** | −5.14** | −11.60*** | −10.38*** | 0.27 | −12.37*** |

*Note.* This table reports test statistics for the augmented Dickey-Fuller (ADF), Phillip–Perron (PP), Kwiatowski-Pillips-Schmidt-Shin (KPSS), and Zivot-Andrews (ZA) unit root test, corresponding to the period 1996:7-2020:10. The tests in levels include only an intercept for the Kilian index, and both an intercept and trend for the other variables. The lag length for the ADF and ZA test are specified based on Schwarz's (1978) information criterion with a maximum of 12 lags, following the suggestion of Pesaran and Shin (1995). For the PP and KPSS test, the lag length is selected with the plug-in procedure of Newey and West (1994) using the Bartlett kernel. 'ln' indicates that the respective variable is transformed to natural logarithms. ** and *** indicate significance at a 5% and 1% significance level, respectively.

For this end, various popular parametric tests are used. More precisely, we apply the augmented Dickey-Fuller (ADF; Dickey and Fuller, 1981), Phillip–Perron (PP; Phillips and Perron, 1988), Kwiatowski-Pillips-Schmidt-Shin (KPSS; Kwiatkowski et al., 1992), and Zivot-Andrews (ZA; Zivot and Andrews, 2002) unit root test. Under the null hypothesis, the ADF, PP, and ZA test assume that a certain process has a unit root and is thus non-stationary, whereas the null hypothesis for the KPSS test states that the respective time series is stationary. In addition, the ZA test is robust to a one-time structural break, while the other tests are known to have low power in the presence of such a break (see Perron, 1989, e.g.). Together, the four tests thus provide us with a thorough understanding of the stationary properties of the time series.

The test statistics are reported in Table 1, computed for both the levels and first differences of all variables. Generally, the unit root tests agree on the integration order of the series, illustrating that most variables are stationary after first differencing. A notable exception is the Kilian index, which appears to be integrated of order zero. Interestingly, contrary to what the other three tests suggest, based on the ZA test we conclude that the natural gas price and CPI are also stationary in levels. This underlines the importance of accounting for a structural break in the series when testing for a unit root. Overall, we find evidence that the variables used in our study are of mixed orders of integration, i.e., $I(0)$ and $I(1)$. This implies that there may exist cointegrating or long-run relationships among the variables, which we will discuss in more detail in the upcoming section.

# 3 Methodology

This section presents the empirical approach used to analyze the dynamic relationship between of each the commodity price series and global climate policy uncertainty. Section 3.1 introduces a flexible framework that allows for simultaneous modeling of long-run relations and short-run dynamics. In Section 3.2, we outline the proposed estimation procedure. Section 3.3 elaborates on the causal links among the variables under study. Finally, we discuss the economic value of our methodology in Section 3.4.

## 3.1 Dynamic Framework

### 3.1.1 ARDL Model

To describe the evolution of commodity prices over time, literature has popularized the use of dynamic models that intend to reproduce some of the characteristics of commodity prices, such as their high degree of persistence (Deaton and Laroque, 1992). Here, prices are commonly related to a set of macroeconomic variables that proxy for market-wide forces. In this context, besides short-run dynamics, numerous studies have pointed out the importance of taking into account long-run equilibrium relations (see He et al., 2010; Schwartz and Smith, 2000, e.g.). Indeed, the results of the unit root tests suggest that there may exist a common stochastic trend among each of the commodity price series, the global CPU factor, and the control variables. Given the aim of our research—i.e., to investigate the impact of a change or shock in global uncertainty on commodity prices—it is therefore imperative to examine both short-term dependencies and longer-term cointegrating relationships.

We perform our analysis within a simple autoregressive distributed lag (ARDL) framework (Pesaran, 1997; Pesaran and Shin, 1995). The ARDL model specifies a single reduced-form equation that relates the dependent variable to its past realizations, as well as current and past realizations of a set of regressors. Suppressing the index for the commodity, let $y_t$ be the natural logarithm of the futures price in month $t \in \{1, \dots, T\}$ of one of the commodities introduced in Section 2.2, $u_t$ the global climate policy uncertainty index, and $z_t = (\text{Kilian}_t, \ln \text{MSCI}_t, \text{LIBOR}_t, \ln \text{FX}_t, \ln \text{CPI}_t)'$ the vector collecting the control variables. The long-run relationship between the price series and the independent variables is then specified as

$$y_t = \alpha + \beta u_t + \gamma' z_t + \varepsilon_t, \tag{3}$$

with the corresponding unrestricted error correction representation of the ARDL$(p, q)$ model given by

$$\Delta y_t = c + \rho y_{t-1} + \theta u_{t-1} + \theta_z' z_{t-1} + \sum_{j=1}^{p-1} \varphi_j \Delta y_{t-j} + \sum_{j=0}^{q-1} \left( \pi_j \Delta u_{t-j} + \pi_{z,j}' \Delta z_{t-j} \right) + e_t, \tag{4}$$

where it is assumed that $y_t$ is an $I(1)$ variable and none of the independent variables is $I(2)$. In this model, the coefficients $\theta$ and $\theta_z$ represent the equilibrium effects of the uncertainty index and control variables, respectively, while $\rho$ is the speed-of-adjustment coefficient indicating the rate at which the commodity price converges towards the equilibrium after a change in the exogenous variables. The coefficients of the differenced

components account for short-run fluctuations not due to deviations from the long-run trend. We can estimate the model straightforwardly by ordinary least squares (OLS).

Several alternative methods to deal with non-stationary time series have been proposed in the literature (see Shrestha and Bhatta, 2018, for an overview). For instance, some studies simply transform non-stationary variables to stationary ones by means of first differencing or by applying the Hodrick Prescott filter to extract long-term trends and cycles. The analysis then proceeds as in the case of stationary time series, e.g., using OLS or VAR models to analyze the relationship of interest. However, any information regarding long-run relations contained in the series is lost when adopting such an approach. If all variables under study are non-stationary, another option is to test for the existence of such a long-run equilibrium using standard cointegration tests (Johansen, 1988; Johansen and Juselius, 1990). In case a cointegrating relation is established, the vector error correction model (VECM) can be derived. Nevertheless, as noted by Shrestha and Bhatta (2018), these cointegration methods and the VECM approach require all time series to be $I(1)$. The evidence of mixed orders of integration found in Section 2.4 suggests that they are thus not applicable given our data.

Once the model specified in Equation (4) is estimated, we can employ the bounds testing approach of Pesaran et al. (2001) to test for the existence of a long-run cointegrating relationship between $y_t$, $u_t$, and $z_t$. This approach involves two tests on the coefficients of the lagged level terms. First, we use an $F$-test for the joint null $H_0 : \rho = \theta = \theta_z = 0$. As Pesaran et al. (2001) point out, in two degenerate cases significance of the overall $F$-test does not imply cointegration. Therefore, as second test the $t$-statistic of Banerjee et al. (1998) is used for the null hypothesis of no cointegration $H_0 : \rho = 0$ against the alternative of cointegration $H_1 : \rho < 0$. This way, we assess whether significance of the $F$-test is perhaps due solely to the lagged levels of the independent variables, which would indicate a degenerate lagged dependent variable. To rule of the case of degenerate lagged independent variables, Pesaran et al. (2001) make the assumption that the dependent variable is $I(1)$. Instead, we augment the bounds testing approach with an $F$-test on the joint significance of the lagged independent variables ($H_0 : \theta = \theta_z = 0$), in line with the recent suggestion of Sam et al. (2019). This additional test allows us to relax the assumption of an $I(1)$ dependent variable, such that we need not rely on the unit root testing results for the price series. If the null hypotheses of all three tests are rejected, we conclude that a long-run equilibrium relationship exists among the variables.

The bounds testing approach to cointegration has several key advantages over traditional cointegration techniques, such as that of Engle and Granger (1987) and Johansen (1988). Namely, as highlighted by Duasa (2007), for example, the procedure of Pesaran et al. (2001) can be used regardless of whether the exogenous variables are purely $I(0)$, purely $I(1)$, or a mixture of both. Moreover, even when the unit root tests would suggest that the variables are of the same integration order, there is still uncertainty associated with the specification of integration orders. As long as none of the independent variables is $I(2)$, the bounds testing approach of Pesaran et al. (2001) does not require such pre-testing. Furthermore, ARDL models and consequently the bounds testing approach allow for varying optimal lag orders of the variables, contrary to standard VAR- or VECM-based cointegration methods.

### 3.1.2 Nonlinear Dependencies

The model specified in Equation (4) assumes symmetry in the relationship between each of the commodity price series and the exogenous variables. With respect to climate policy uncertainty, this means that, in absolute terms, an increase in global uncertainty affects commodity prices in the same way as a decrease of equal magnitude. Yet, literature provides ample evidence that such a symmetry constraint may be too restrictive. Generally, the impact of positive uncertainty shocks on economic outcomes tends be greater than that of negative shocks (Grier et al., 2004; You et al., 2017). In this case, a sudden increase in uncertainty need not be offset by subsequent decreases, such that the effects of positive spikes may be long-lasting.

Within the ARDL framework, Shin et al. (2014) demonstrate that we can accommodate asymmetries in both the underlying long-run relationship and dynamic adjustment patterns through partial sum decompositions of the exogenous variables. The resulting nonlinear ARDL (NARDL) model enables us to examine potential differences in the impact of negative and positive CPU shocks on the commodity prices. Using the notation introduced before, we specify the asymmetric long-run relationship as

$$y_t = \alpha + \beta^+ u_t^+ + \beta^- u_t^- + \gamma' z_t + \varepsilon_t, \tag{5}$$

where the partial sum processes $u_t^+$ and $u_t^-$ of positive and negative changes in $u_t$, respectively, are defined as

$$u_t^+ = \sum_{t=1}^{T} \Delta u_t^+ = \sum_{t=1}^{T} \max(\Delta u_t, 0) \quad \text{and} \quad u_t^- = \sum_{t=1}^{T} \Delta u_t^- = \sum_{t=1}^{T} \min(\Delta u_t, 0),$$

such that $u_t = u_0 + u_t^+ + u_t^-$. Here, a known threshold value of zero is assumed, enabling economic interpretation of the model.[6] In this model, we impose a linear or symmetric impact of the control variables on the commodity price, which Shin et al. (2014) refer to as partial asymmetry. Namely, the control variables are not the primary focus and this linearity assumption significantly reduces the dimension of the estimated NARDL models, thereby facilitating statistical inference. The unrestricted error correction respresentation of the NARDL$(p, q)$ model associated with the long-run relationship in Equation (5) is given by

$$\begin{aligned} \Delta y_t = c + \rho y_{t-1} + \theta^+ u_{t-1}^+ + \theta^- u_{t-1}^- + \theta_z' z_{t-1} \\ + \sum_{j=1}^{p-1} \varphi_j \Delta y_{t-j} + \sum_{j=0}^{q-1} \left( \pi_j^+ \Delta u_{t-j}^+ + \pi_j^- \Delta u_{t-j}^- + \pi_{z,j}' \Delta z_{t-j} \right) + e_t, \end{aligned} \tag{6}$$

which is again estimable by OLS.

To establish whether a long-run equilibrium relationship exists between $y_t$, $u_t^+$, $u_t^-$, and $z_t$, we can employ the three tests comprising the bounds testing approach outlined above. Although the control variables enter the long-run equation in symmetric form, in the remainder of this paper we will refer to this cointegrating relation as nonlinear. As explained by Shin et al. (2014), the idea that the equilibrium relationship may involve the partial sum components of an exogenous variable rather than the underlying variable itself is

[6] This decomposition of the global uncertainty factor leads to a split of positive and negative changes in $u_t$ of around 50:50.

closely related to concept of 'hidden cointegration' developed by Granger and Yoon (2002). In particular, Granger and Yoon (2002) argue that the components of economic series—i.e., either the positive or negative components—may contain valuable information to help understand the dynamic relationship of interest, which could go undetected when analyzing linear cointegration.

Regarding the models capable of dealing with non-stationary time series, several alternatives are available to address the issue of nonlinearity (see Shin et al., 2014). The most popular of such models are regime-switching models, such as the smooth transition or Markov-switching ECM (Kapetanios et al., 2006; Psaradakis et al., 2004). However, contrary to these models, the NARDL approach jointly estimates cointegration and asymmetries. Additionally, in the regime-switching models asymmetries are generally limited to the error correction mechanism, thereby neglecting nonlinearities in the long-run equilibrium relations. The NARDL approach, on the other hand, encompasses all four combinations of long-run and short-run (a)symmetry. Moreover, standard tests can be used to obtain the appropriate model specification. This flexibility is a key feature of the NARDL model.

#### 3.1.3 Testing for Symmetry

The NARDL model specified in Equation (6) is general in the sense that it incorporates both asymmetry in the long-run relationship and short-run adjustment asymmetry. In fact, based on this model specification we can distinguish numerous forms of asymmetry, for which we can test in order to determine the appropriate specification for each commodity (Shin et al., 2014). Regarding the long run, inequality of the coefficients of $u_t^+$ and $u_t^-$ in Equation (5) implies asymmetry in the long-run impact of positive and negative changes in global CPU on the price series. These parameters are often referred to as the long-run multipliers and are obtained as $\beta^+ = -\theta^+/\rho$ and $\beta^- = -\theta^-/\rho$. The estimation results of Equation (6) can then be used to compute the Wald statistic for the null hypothesis of long-run or reaction symmetry $H_0 : \beta^+ = \beta^-$.

With respect to the short run, we can test for two forms of symmetry: pair-wise symmetry and additive symmetry. The former implies that for all $j = 0, \ldots, q-1$, the short-run parameters $\pi_j^+$ and $\pi_j^-$ are equal. In this case, the short-run adjustment patterns of a commodity price to positive and negative shocks in uncertainty will be exactly symmetrical. Since this form of short-run symmetry is rather restrictive, we do not explicitly test for it. Instead, differences in the lag structures of $\Delta u_t^+$ and $\Delta u_t^-$ directly indicate asymmetry in the patterns of adjustment. Additive symmetry, on the other hand, means that positive and negative changes in an exogenous variable have the same (absolute) summative short-run impact on the dependent variable. We assess this form of symmetry by means of the Wald test for the null hypothesis $H_0 : \sum_{j=0}^{q-1} \pi_j^+ = \sum_{j=0}^{q-1} \pi_j^-$. If none of the forms of symmetry is rejected, the NARDL model reduces to the linear ARDL model of Pesaran and Shin (1995).

### 3.1.4 Cumulative Dynamic Multipliers

To visualize the adjustment patterns over time of the dependent variable to positive and negative shocks in one of the exogenous variables, Shin et al. (2014) evaluate the cumulative dynamic multiplier effects. Similar to impulse response functions for VAR models, the dynamic multipliers allow us to trace out how each price series reacts to changes in global climate policy uncertainty. As noted by Shin et al. (2014), the exact adjustment pattern will depend on the combination of long-run parameters, speed of adjustment, and short-run dynamics.

The cumulative dynamic multiplier effects of $u_t^+$ and $u_t^-$ on $y_t$ are defined as

$$m_h^+ = \sum_{j=0}^{h} \frac{\partial y_{t+j}}{\partial u_t^+} = \sum_{j=0}^{h} \boldsymbol{\lambda}_j^+ \quad \text{and} \quad m_h^- = \sum_{j=0}^{h} \frac{\partial y_{t+j}}{\partial u_t^-} = \sum_{j=0}^{h} \boldsymbol{\lambda}_j^-, \quad h = 0, 1, 2, \ldots,$$

where it holds that $m_h^+ \to \beta^+$ and $m_h^- \to \beta^-$ as $h \to \infty$. The dynamic multipliers $\boldsymbol{\lambda}_j^+$ and $\boldsymbol{\lambda}_j^-$ can be obtained based on the parameters of the levels representation of the NARDL$(p, q)$ model, which in turn are derived from the parameters in Equation (6). In particular, the parameters of the lags of $y_t$ are equal to $\phi_1 = \rho + 1 + \varphi_1, \phi_j = \varphi_j - \varphi_{j-1}, j = 2, \ldots, p-1$, and $\phi_p = -\varphi_{p-1}$. The level parameters corresponding to (the lags of) $u_t^+$ and $u_t^-$ are equal to $\theta_0^l = \pi_0^l, \theta_1^l = \theta^l - \pi_0^l + \pi_1^l, \theta_j^l = \pi_j^l - \pi_{j-1}^l, j = 2, \ldots, q-1$, and $\theta_q^l = -\pi_{q-1}^l$, $l = +, -$. Finally, the dynamic multipliers are determined using the following recursion:

$$\boldsymbol{\lambda}_j^l = \phi_1 \boldsymbol{\lambda}_{j-1}^l + \phi_2 \boldsymbol{\lambda}_{j-2}^l + \ldots + \phi_{j-1} \boldsymbol{\lambda}_1^l + \phi_j \boldsymbol{\lambda}_0^l + \theta_j^l, \quad l = +, -, \quad j = 1, 2, \ldots,$$

with $\boldsymbol{\lambda}_0^l = \theta_0^l, \phi_j = 0$ for $j < 1$, and $\boldsymbol{\lambda}_j^l = 0$ for $j < 0$.

## 3.2 Two-Step Estimation Procedure

As mentioned before, the NARDL model of Shin et al. (2014) specified in Equation (6) is estimable by OLS, after which the long-run coefficients $\beta^+, \beta^-$, and $\gamma$ are obtained by a simple transformation of the parameter estimates. However, by construction, the partial sum decompositions $u_t^+$ and $u_t^-$ exhibit deterministic time trends that are asymptotically perfectly collinear. While Shin et al. (2014) have established the efficacy of their single-step OLS estimator using Monte Carlo simulations, this collinearity introduces a singularity problem that hampers the development of the corresponding asymptotic theory.

Addressing the asymptotic singularity associated with the single-step estimator, Cho et al. (2020) have recently proposed a two-step estimation framework for the NARDL model, along the lines of Engle and Granger (1987). In the first step, the fully modified OLS (FM-OLS) estimator of Phillips and Hansen (1990) is used to estimate the parameters of the long-run relationship, which is robust to both endogeneity of the regressors and serial correlation. Moreover, the estimator follows a known asymptotic distribution, thereby allowing for standard inference. Subsequently, the dynamic parameters are estimated by OLS conditional on the long-run coefficients. A key feature of this approach is that it is analytically tractable, enabling Cho et al. (2020) to derive the limit distributions of the estimators. As indicated by Bahmani-Oskooee et al. (2020), because of the advantages of this novel approach, future research should move towards two-step estimation of NARDL models.

Therefore, a comparison of the empirical performance of the one-step and two-step estimation approach would be particularly useful.

Accordingly, we adopt the two-step estimation approach. However, Cho et al. (2020) solely focus on the cases with $k = 1$ and $k > 1$ decomposed independent variables, whereas in our analysis we consider both the decomposed global CPU factor and a set symmetric control variables. For this purpose, we extend the case with one decomposed or asymmetric variable to also incorporate a set of $n$ variables that enter the model in symmetric form. The details of the procedure are presented below, largely following the notation of Cho et al. (2020). For all proofs and more details on the derivations, we refer to Cho et al. (2020).

#### 3.2.1 Step 1: Long-Run Parameters

We begin by rewriting the long-run relationship specified in Equation (5) as

$$y_t = \alpha + \lambda u_t^+ + \eta u_t + \gamma' z_t + \varepsilon_t, \tag{7}$$

where $\lambda = \beta^+ - \beta^-$ and $\eta = \beta^-$. This transformation resolves the singularity issue resulting from the collinear time trends in $u_t^+$ and $u_t^-$, thus facilitating inference. Defining the vector $q_t := (1, u_t^+, u_t, z_t')'$, the parameters $\varrho := (\alpha, \lambda, \eta, \gamma')'$ in Equation (7) are estimated by OLS as

$$\widehat{\varrho} := (\widehat{\alpha}, \widehat{\lambda}, \widehat{\eta}, \widehat{\gamma}')' := \left(\sum_{t=1}^{T} q_t q_t'\right)^{-1} \left(\sum_{t=1}^{T} q_t y_t\right) = \varrho + \left(\sum_{t=1}^{T} q_t q_t'\right)^{-1} \left(\sum_{t=1}^{T} q_t \varepsilon_t\right),$$

from which the long-run multipliers are derived as $\widehat{\beta}^+ = \widehat{\lambda} + \widehat{\eta}$ and $\widehat{\beta}^- = \widehat{\eta}$.

Next, FM-OLS is used to correct the OLS estimator $\widehat{\varrho}$ for any asymptotic bias caused by endogeneity of the regressors and/or serial correlation in the residuals $\varepsilon_t$. Specifically, we follow Newey and West (1987) to obtain a heteroskedasticity and autocorrelation consistent estimate of the covariance matrix associated with the last component in the expression for $\widehat{\varrho}$ above:

$$\widetilde{\Sigma} := \begin{bmatrix} \widetilde{\Sigma}^{(1,1)} & \widetilde{\sigma}^{(1,2)} \\ \widetilde{\sigma}^{(2,1)} & \widetilde{\sigma}^{(2,2)} \end{bmatrix} := \frac{1}{T}\sum_{t=1}^{T} \widehat{g}_t \widehat{g}_t' + \frac{1}{T}\sum_{k=1}^{L} w_k \sum_{t=k+1}^{T} \{\widehat{g}_{t-k}\widehat{g}_t' + \widehat{g}_t \widehat{g}_{t-k}'\},$$

where $\widehat{g}_t := (\Delta u_t, \Delta z_t', \widehat{\varepsilon}_t)'$, $w_k := 1 - k/(1+L)$, $L := T^{1/4}$, and $\widehat{\varepsilon}_t := y_t - \widehat{\alpha} - \widehat{\beta}^+ u_t^+ - \widehat{\beta}^- u_t^- - \widehat{\gamma}' z_t$. Furthermore, to arrive at a consistent estimate of the asymptotic bias $v$, the following matrix is defined:

$$\widetilde{\Pi} := \begin{bmatrix} \widetilde{\Pi}^{(1,1)} & \widetilde{\pi}^{(1,2)} \\ \widetilde{\pi}^{(2,1)} & \widetilde{\pi}^{(2,2)} \end{bmatrix} := \frac{1}{T}\sum_{k=0}^{L} \sum_{t=k+1}^{T} \widehat{g}_{t-k} \widehat{g}_t'.$$

Here, as illustrated by Cho et al. (2020), the definition of $\pi^{(1,2)}$ is identical to $v$. The FM-OLS estimator of the long-run parameters is then given by

$$\widetilde{\varrho} := (\widetilde{\alpha}, \widetilde{\lambda}, \widetilde{\eta}, \widetilde{\gamma}')' := \left(\sum_{t=1}^{T} q_t q_t'\right)^{-1} \left(\sum_{t=1}^{T} q_t \widetilde{y}_t - T S' \widetilde{v}\right),$$

where $\widetilde{y}_t := y_t - l_t' (\widetilde{\Sigma}^{(1,1)})^{-1} \widetilde{\sigma}^{(1,2)}$, $l_t := (\Delta u_t, \Delta z_t')'$, $\widetilde{v} := \widetilde{\pi}^{(1,2)} - \widetilde{\Pi}^{(1,1)} (\widetilde{\Sigma}^{(1,1)})^{-1} \widetilde{\sigma}^{(1,2)}$, and $S := [0_{(n+1)\times 2}, I_{n+1}]$. Again, a simple transformation yields the estimates of the long-run multipliers: $\widetilde{\beta}^+ = \widetilde{\lambda} + \widetilde{\eta}$ and $\widetilde{\beta}^- = \widetilde{\eta}$.

### 3.2.2 Step 2: Short-Run Parameters

Cho et al. (2020) argue that the estimates of the long-run parameters of the first step are super-consistent, converging at a rate of $T$. Therefore, the parameters can be treated as known in the second step, in which the dynamic coefficients are estimated. To this end, we define the error correction term

$$\varepsilon_{t-1} := y_{t-1} - \alpha - \beta^+ u^+_{t-1} - \beta^- u^-_{t-1} - \gamma' z_{t-1},$$

and rewrite Equation (6) in conditional error correction form as

$$\Delta y_t = c + \rho \varepsilon_{t-1} + \sum_{j=1}^{p-1} \varphi_j \Delta y_{t-j} + \sum_{j=0}^{q-1} \left( \pi^+_j \Delta u^+_{t-j} + \pi^-_j \Delta u^-_{t-j} + \pi'_{z,j} \Delta z_{t-j} \right) + e_t. \tag{8}$$

The short-run parameters can then be obtained by OLS, since all variables in the equation are stationary. Particularly, if $\zeta := (c, \rho, \varphi_1, \ldots, \varphi_{p-1}, \pi^+_0, \pi^+_1, \ldots, \pi'_{z,q-1})'$ is the parameter vector corresponding to Equation (8) and $h_t$ the vector collecting the realizations of the regressors, the dynamic coefficients are estimated as

$$\widehat{\zeta} := \left( \sum_{t=1}^{T} h_t h_t' \right)^{-1} \left( \sum_{t=1}^{T} h_t \Delta y_t \right).$$

### 3.2.3 Testing for Symmetry

Lastly, we describe the Wald testing approach developed by Cho et al. (2020) to assess the significance of asymmetries in the long run and short run. Regarding the former, we are interested in the null hypothesis of symmetry $H_0 : \beta^+ = \beta^-$ against the alternative $H_1 : \beta^+ \neq \beta^-$. Noting that $\beta^+ - \beta^- = \lambda$, this is equivalent to testing $H_0' : R_l \varrho = r$ against $H_1' : R_l \varrho \neq r$, with $r = 0$ and selection vector $R_l := (0, 1, 0, 0_{1\times n})$. Given the FM-OLS estimator $\widetilde{\varrho}$, the corresponding Wald test statistic is computed as

$$\mathcal{W}_l := (R_l \widetilde{\varrho} - r)' (\widetilde{\tau}^2 R_l Q^{-1} R_l')^{-1} (R_l \widetilde{\varrho} - r),$$

where $\widetilde{\tau}^2 := \widetilde{\sigma}^{(2,2)} - \widetilde{\sigma}^{(2,1)} (\widetilde{\Sigma}^{(1,1)})^{-1} \widetilde{\sigma}^{(1,2)}$ and $Q := \sum_{t=1}^{T} q_t q_t'$. Because the limit distribution of the FM-OLS estimator $\widetilde{\varrho}$ is mixed normal, $\mathcal{W}_l$ asymptotically follows a $\chi^2$-distribution with one degree of freedom under the null hypothesis.

Similarly, a Wald statistic is constructed to test for additive symmetry of the short-run parameters, where we consider the null hypothesis $H_0 : R_s \zeta = r$ against the alternative $H_1 : R_s \zeta \neq r$. Again, we set $r = 0$ and define selection vector $R_s := (0_{1\times(1+p)}, \iota_q', -\iota_q', 0_{1\times q})$. Conditional on $\widehat{\zeta}$, the test statistic is then given by

$$\mathcal{W}_s := T (R_s \widehat{\zeta} - r)' (R_s \widehat{\Gamma}^{-1} \widehat{\Omega} \widehat{\Gamma}^{-1} R_s')^{-1} (R_s \widehat{\zeta} - r),$$

where $\widehat{\Omega} := T^{-1} \sum_{t=1}^{T} \widehat{e}_t^2 h_t h_t'$ is a heteroskedasticity consistent covariance estimator, $\widehat{e}_t := \Delta y_t - \widehat{\zeta}' h_t$, and $\widehat{\Gamma} := T^{-1} \sum_{t=1}^{T} h_t h_t'$. Under the null, $\mathcal{W}_s$ follows an asymptotic $\chi^2$-distribution with one degree of freedom.

### 3.3 Granger Causality

The methodology introduced in the previous sections focuses on the dynamic relation between the commodity price series and global climate policy uncertainty. However, it does not address the issue of causality (Granger, 1969). While in a cointegrated bivariate system there must be causality in at least one direction (Engle and Granger, 1987), due to the multivariate nature of our analysis, the existence of a cointegrating relation does not directly imply a causal link between the CPU factor and any of the commodity prices. Moreover, there may be a causal relation between two time series even in the absence of cointegration. It is therefore essential to investigate the existence and direction of causality in the relationship between (the partial sum processes of) the global climate policy uncertainty index and each of the commodity prices. Namely, it is only appropriate to draw conclusions about the impact of a shock in global uncertainty on the price of a certain commodity once a causal link from the former to the latter has been established. Without causality, the results of the empirical analysis should be interpreted in terms of associations, and neglecting this would lead to partial or misleading conclusions.

In general, testing for Granger causality involves testing zero restrictions on specific coefficients in a VAR model. However, as emphasized by Lütkepohl (2005), the limit distribution of the corresponding Wald statistic is non-standard in the presence of non-stationary time series. Accordingly, we employ the causality testing procedure developed by Toda and Yamamoto (1995), which is valid irrespective of the integration order of the considered variables. Moreover, combining the procedure with the concept of partial sum decompositions allows us to test for asymmetric causal relationships, similar to the approach of Hatemi-J (2012).

The procedure of Toda and Yamamoto (1995) consists of two steps. In the first step, we specify a VAR($k$) model in levels including the price $y_t$ of one of the commodities, the partial sum processes $u_t^+$ and $u_t^-$ associated with the CPU factor, and the control variables $z_t$. The lag length $k$ is chosen according to some information criterion, increasing the number of lags in case the residuals are serially correlated. Subsequently, the VAR model is augmented with $d_{max}$ lags, where $d_{max}$ is equal to the maximum integration order found among the variables in $Y_t = (y_t, u_t^+, u_t^-, z_t')'$. Setting $p = k + d_{max}$, we thus estimate the following VAR($p$) model:

$$Y_t = a_0 + \sum_{j=1}^{k} A_j Y_{t-j} + \sum_{j=k+1}^{p} A_j Y_{t-j} + \varepsilon_t. \tag{9}$$

The causal relationship between the uncertainty factor and $y_t$ is then examined using standard tests on the elements of $A_1, \ldots, A_k$. Specifically, if $a_{j,lr}$ is the $(l,r)$-th element of $A_j$, we test whether $u_t^+$ Granger causes $y_t$ by computing the Wald statistic for the null hypothesis of no causality $H_0 : a_{1,12} = a_{2,12} = \ldots = a_{k,12} = 0$. Similarly, we are able to test for a causal link from $u_t^-$ to $y_t$, or from $y_t$ to $u_t^+$ or $u_t^-$—that is, reverse causality. In this procedure, the $d_{max}$ additional lags are solely included in the VAR model to ensure that the Wald test statistics asymptotically follow the usual $\chi^2$-distribution (Toda and Yamamoto, 1995)

### 3.4 Forecasting Exercise

Lastly, to assess the economic value of our research, in this section we outline a simple forecasting exercise. According to the arbitrage pricing theory of Ross (1976), the expected return on an asset can be approximated by a linear combination of systemic risk factors. Consequently, given climate-related regulatory uncertainty as a potential source of risk for investors participating in commodity markets, commodity allocations may be hurt by unintended exposure to the CPU factor. In this case, identification of a relevant climate risk factor and an accurate understanding of its relationship with commodities should help predict commodity prices and provide practitioners economic merit.

The goal of this exercise is to examine the accuracy of the commodity price forecasts produced by the NARDL model, particularly when employing the two-step estimation procedure of Cho et al. (2020). Whereas previously we mainly posed arguments in favor of this procedure related to asymptotic theory, by comparing these forecasts to those obtained using the conventional one-step NARDL approach we are able to quantify differences in economic performance. Such a comparison is especially relevant, as the approach of Cho et al. (2020) is a relatively recent advancement and no empirical applications are available yet in the literature. To evaluate the relative performance of the NARDL-based approaches, we consider two benchmark models: the random walk (RW) with drift and the linear ARDL model. The former is estimated in levels and sets all forecasts equal to the last observed value plus a drift term. Despite its simplicity, forecasts produced by the RW model are generally hard to beat in terms of accuracy (see Meese and Rogoff, 1983; Taylor, 1995, e.g.), thereby serving as an important benchmark in empirical asset pricing. On the other hand, the linear ARDL model provides a useful benchmark since it allows us to establish whether taking into account the asymmetric impact of uncertainty shocks yields superior economic performance.

Numerous studies have emphasized that adequate modeling of error correction mechanisms is crucial for constructing reliable forecasts in cointegrated systems, particularly at medium- and long-term forecasting horizons (Engle and Granger, 1987; Hoffman and Rasche, 1996). Accordingly, as our empirical framework encompasses both short-run dynamics and long-run equilibrium relations, we compute commodity price forecasts at various horizons. More precisely, for each commodity we generate pseudo out-of-sample futures price forecasts for one to twelve months ahead. Here, we compute ex-post forecasts, meaning that actual values of the independent variables are used instead of predicted values in case the forecasting equation requires observations of the regressors that fall outside of the estimation period. This choice is motivated by the fact that our primary objective is to conduct a preliminary investigation of the properties of the competing forecasting models. Incorporating predicted independent variables would introduce additional uncertainty into each forecasting model—except for the RW model—that is not necessarily related to the model itself, and may therefore distort comparison. Moreover, predicting economic variables such as the 3-month LIBOR and the U.S. nominal effective exchange rate is a considerable task, that is outside the scope of this study.

# 4 Results

In this section, we study the dynamic relation between the monthly commodity futures prices introduced in Section 2.2 and the global climate policy uncertainty index described in Section 2.1. We present and discuss the long-run and short-run estimation results in Section 4.1 and 4.2, respectively. In Section 4.3, we examine the causal links between the variables under study, while Section 4.4 visualizes the dynamic adjustment patterns. Finally, in Section 4.5 we evaluate and comment on the economic implications of our methodology.

## 4.1 Long-Run Relationships

First, we apply the methods outlined in the previous section to investigate the existence of cointegrating relationships and determine the associated long-run parameters. The sample period ranges from July 1996 to October 2020, constituting $T = 292$ monthly observations. The starting point of our empirical analysis is the general NARDL model, rather than the more restrictive ARDL model. Namely, the former accommodates all combinations of long-run and short-run (a)symmetry, where the ARDL model is obtained in the special case of symmetry in both the long run and short run. This way, we are able to test for the correct symmetry specification for each commodity, instead of running the risk of obtaining misleading linear estimation results in case the underlying relation is in fact asymmetric (Shin et al., 2014).

As discussed in Section 3.2, the recently developed two-step estimation procedure of Cho et al. (2020) is employed to estimate the NARDL models. For comparative purposes, the models are also estimated by OLS in the single-step framework adopted by Shin et al. (2014). With respect to the former, we have modified the procedure slightly. Specifically, we have extended the case with one decomposed independent variable to accommodate both asymmetric variables—in the form of the partial sum decompositions $u_t^+$ and $u_t^-$ of the global CPU factor—and symmetric variables, namely the control variables $z_t$. To examine whether the two-step estimator and the corresponding Wald test statistics continue to have adequate finite sample performance, we perform various Monte Carlo simulations. Details on the data generating processes and simulation results are presented in Appendix E. In the simulations, a range of values of $\varphi$ is considered to investigate the sensitivity of the results to the degree of serial correlation. First, we observe that the finite sample bias and mean squared error of the parameter estimates converge to zero relatively quickly when the sample size increases. This holds true for all values of $\varphi$, demonstrating the satisfactory performance of the two-step approach.[7] Regarding the Wald tests, the empirical levels indicate that the test statistic for short-run symmetry is adequately approximated by a $\chi^2$-distribution with one degree of freedom, even in limited samples. However, it appears that the test for long-run symmetry is slightly mis-sized, especially when $\varphi$ is below zero. This observations is in line with that of Shin et al. (2014) and Cho et al. (2020), who suggest the use of empirical $p$-values in

[7] Similar to Cho et al. (2020), we find that the two-step estimator is considerably more efficient and less biased when FM-OLS is used in the first step compared to OLS, illustrating the relevance of the endogeneity and autocorrelation robust estimation approach. Given the primary focus of our study and to conserve space, we do not report simulation results for the case where the long-run relationship in the first step is estimated by OLS.

small samples. Lastly, the empirical results for the power of the Wald tests support the consistency of the test statistics under the alternative hypothesis, approaching 100% for all values of $\varphi$ as the sample size increases. Altogether, the simulation results demonstrate the validity of the modified two-step estimation procedure.

To determine the final NARDL model specifications, a general-to-specific modeling approach is used (Hendry, 1995; Shin et al., 2014). While the appropriate lag orders of the regressors in ARDL models are commonly specified based on information criteria (see Pesaran et al., 2001, e.g.), the general-to-specific procedure has important advantages. For instance, suppose that we set the maximum lag order equal to 12, in line with the general recommendation of practitioners for monthly data (Ivanov et al., 2001). Then, given the number of exogenous variables, deriving the optimal lag structure using information criteria would require us to evaluate around $12 \times 13^7 \approx 750$ million model configurations for each commodity, posing a severe computational burden. In addition, as pointed out by Katrakilidis and Trachanas (2012) in the context NARDL models, including insignificant lags tends make inference less accurate and could lead to noise in the estimation of the dynamic multipliers. We therefore advocate the use of a general-to-specific approach, where the starting point is a NARDL model with a maximum lag order of 12 and the dynamic regressor with the highest $p$-value is dropped sequentially. Here, we use a 5% unidirectional decision rule and continue until all short-run dynamic coefficients are significant, resulting in a more parsimonious model.[8]

Before estimating the long-run multipliers, we focus on NARDL bounds testing for nonlinear cointegration (Shin et al., 2014). That is, we test for the existence of an asymmetric long-run relationship between each of the price series, the global level of CPU, and the control variables. Here, we include an unrestricted intercept in the error correction representation of the NARDL model, as in Equations (6) and (8), accounting for a drift in the commodity price series. The corresponding critical values are obtained from Pesaran et al. (2001), who specify one set of values for the case where the independent variables are purely $I(0)$ and one for the case where they are purely $I(1)$. Together, these sets provide critical value bounds for the cointegration test that can be used irrespective of the integration order of the regressors. However, the results of this approach are only conclusive if the test statistic falls outside of the bounds. Otherwise, they are inconclusive and more details may be needed regarding the exact orders of integration. Furthermore, because of the dependence structure between the partial sum processes $u_t^+$ and $u_t^-$, the precise number of exogenous variables used to determine the critical values is unknown (Shin et al., 2014). To prevent premature rejection of the null hypotheses, the partial sums are counted as a single regressor, leading to more conservative testing.

Table 2 presents the statistics of the three tests comprising the bounds testing approach described in Section 3.1.1, as well as the LM statistic of the Breusch-Godfrey test for serial correlation in the residuals. The

[8] In Section 2.4, the Zivot-Andrews test suggested a structural break in the natural gas price with break date equal to July 2008, corresponding to the 2008 global financial crisis. To account for this break, we specified a dummy variable taking value one over the period 2008:7-2008:12 and zero elsewhere. As mentioned by Pesaran et al. (2001), the inclusion of such a dummy does not affect the asymptotic theory associated with the bounds testing approach. Nonetheless, the dummy was found to be insignificant and consequently dropped in the general-to-specific approach.

Table 2: Bounds Testing for Cointegration

| | One-Step NARDL | | | | Two-Step NARDL | |
|---|---|---|---|---|---|---|
| Commodity | $F_{PSS}$ | $t_{BDM}$ | $F_{IDV}$ | $\chi^2_{SC}$ | $t_{BDM}$ | $\chi^2_{SC}$ |
| Oil | 5.361*** | –6.225*** | 5.383*** | 12.467 | –5.249*** | 7.918 |
| Gas | 5.636*** | –6.376*** | 3.505* | 12.723 | –5.792*** | 11.876 |
| Gold | 4.074** | –4.646** | 4.644** | 13.349 | –5.093*** | 23.995** |
| Copper | 4.113** | –4.748** | 3.914** | 13.762 | –4.480** | 10.826 |
| Sugar | 6.671*** | –6.169*** | 7.044*** | 6.572 | –4.928** | 8.613 |
| Wheat | 6.493*** | –6.045*** | 6.862*** | 15.879 | –5.247*** | 17.022 |

*Note.* This table reports results of the bounds testing approach to nonlinear cointegration proposed by Shin et al. (2014), based on the single-step estimation approach of Shin et al. (2014) and the two-step approach of Cho et al. (2020). Here, we estimate the NARDL models specified in Equations (6) and (8), using a general-to-specific procedure to arrive at the final model specification. We set the maximum lag order equal to 12 and sequentially drop the insignificant dynamic regressors, with a 5% unidirectional decision rule. All equations are estimated including an unrestricted intercept and no trend. $F_{PSS}$ denotes the $F$-statistic of Pesaran et al. (2001), $t_{BDM}$ the $t$-statistic of Banerjee et al. (1998), $F_{IDV}$ the $F$-statistic of Sam et al. (2019), and $\chi^2_{SC}$ the LM statistic of the Breusch-Godfrey test for serial correlation in the residuals up to lag order 12. Critical values of the three bounds tests are derived from Pesaran et al. (2001), where the partial sums $u_t^+$ and $u_t^-$ are counted as a single regressor, resulting in more conservative testing. *, **, and *** indicate significance at a 10%, 5%, and 1% significance level, respectively.

results obtained within the one-step and two-step framework correspond to Equation (6) and (8), respectively. Here, the two-step approach incorporates an error correction term rather than the lagged level terms $y_{t-1}$, $u^+_{t-1}$, $u^-_{t-1}$, and $z_{t-1}$. Therefore, the two $F$-tests are not applicable in this framework, as indicated by Cho et al. (2020). The optimal lag structure of the dynamic regressors is determined using the general-to-specific modeling approach outlined above. Importantly, the results of the two approaches are consistent. In particular, based on the $F_{PSS}$ statistic of Pesaran et al. (2001) we find evidence in favor of a nonlinear cointegrating relationship between each commodity price series and the independent variables. Moreover, the significance of both the $t$-statistic $t_{BDM}$ of Banerjee et al. (1998) and the $F$-statistic $F_{IDV}$ of Sam et al. (2019) in the one-step framework implies an absence of a degenerate lagged dependent variable and degenerate lagged independent variables, respectively (Sam et al., 2019). This means that the significance of $F_{PSS}$ is in fact due to cointegration. The significant $t_{BDM}$ statistics in the two-step approach reinforce this conclusion. Lastly, the $\chi^2_{SC}$ statistics suggests that in general the residuals are serially uncorrelated, which is an essential assumption for the validity of the bounds testing approach (Pesaran et al., 2001). The cointegration results verify the existence of a long-run equilibrium relationship between the prices of each of the six commodities, global climate policy uncertainty, and the control variables.[9] This finding is in line the results obtained by related studies, who generally conclude that commodity prices and macroeconomic variables co-move in the long run (see Ahumada and Cornejo, 2015; Belke et al., 2010, e.g.).

[9] Although not presented here, interesting to note is that the evidence of long-run equilibrium relations is considerably weaker when the CPU factor is omitted from the analysis. For instance, for gold the three test statistics of the bounds testing approach are all insignificant in this case.

Given the cointegration results, we can proceed with inference on the asymmetric long-run parameters $\beta^+$ and $\beta^-$ corresponding to Equation (5). Within the one-step framework, we follow the general-to-specific modeling approach outlined above and obtain the long-run multipliers by the transformation discussed in Section 3.1.3. In the two-step NARDL approach, $\beta^-$ is estimated directly in the first step and $\beta^+$ follows from a linear transformation. The standard errors of the transformed quantities are computed using the Delta method (Bårdsen, 1989).[10] The long-run coefficient estimates are presented in Table 3, together with the Wald test statistic $\mathcal{W}_l$ for long-run symmetry. Comparing the results of the two approaches, we observe differences in both point estimates and standard errors. For example, the estimates obtained from the two-step framework are generally more precise. As observed by Cho et al. (2020), this is likely due to the fact that in the one-step approach the long-run multipliers are recovered as ratios. A denominator—that is, the error correction parameter $\rho$—close to zero or a negative covariance between the numerator and denominator could then result in a loss of precision. Additionally, the discrepancies may be related to the presence of endogeneity and/or serial correlation, which the two-step approach corrects for. Nevertheless, for most commodities the signs of the long-run multipliers are equal across the two approaches. One notable exception is wheat, for which we find negative and significant point estimates in the one-step framework and positive estimates in the two-step approach. This inconsistency illustrates another advantage of the two-step approach, namely that the long-run relationship is modeled separately from the short-run dynamics and hence is not affected by the specified lag structure. Accordingly, for the remainder of the discussion of our empirical analysis we focus our attention on the two-step approach.

The right-hand side of Table 3 offers various key insights regarding the long-run equilibrium relationships under study. First, we observe considerable heterogeneity in the responses of the different commodities to changes in global climate policy uncertainty. As argued by Gospodinov and Jamali (2018), given the distinct characteristics and potential uses of each of the commodities, this is as expected. In particular, we see that the global CPU index and the prices of both oil and gas are negatively related in the long run. Several recent studies investigating the impact of different measures of uncertainty on energy commodities have reached the same conclusion (Huang et al., 2021; Lin and Bai, 2021; Shi and Shen, 2021). Furthermore, the long-run relation between the CPU factor and the gold price is positive. This finding is similar to the results of Bilgin et al. (2018) and Huang et al. (2021), who show a positive response of the gold price to changes in the EPU index of Baker et al. (2016), consistent with the notion of gold as a safe haven. Moreover, the significance of $\mathcal{W}_l$ for oil, gas, and gold indicates asymmetry in the respective long-run relationships. Specifically, the association between global CPU and the prices of the three commodities is stronger for positive changes in uncertainty than for negative changes, in line with the observation made in Section 3.1.2 regarding the asymmetric impact of uncertainty shocks on economic outcomes. Concerning the price of gasoline, Kang et al. (2019) also find such an asymmetric response of the price series to policy uncertainty shocks. Contrarily, for

[10] In particular, in the one-step approach we use that $\text{var}(\hat{\beta}^l) = \hat{\rho}^{-2}[\text{var}(\hat{\theta}^l) + (\hat{\beta}^l)^2\text{var}(\hat{\rho}) + 2\hat{\beta}^l\text{cov}(\hat{\theta}^l, \hat{\rho})]$, $l = +, -$, and in the two-step approach $\text{var}(\tilde{\beta}^+) = \text{var}(\tilde{\lambda}) + \text{var}(\tilde{\eta}) + 2\text{cov}(\tilde{\lambda}, \tilde{\eta})$.

Table 3: Long-Run Coefficient Estimates

| | One-Step NARDL | | | Two-Step NARDL | | |
|---|---|---|---|---|---|---|
| Commodity | $\beta^+$ | $\beta^-$ | $\mathcal{W}_l$ | $\beta^+$ | $\beta^-$ | $\mathcal{W}_l$ |
| Oil | –0.087* | 0.004 | 5.132** | –0.120*** | –0.057** | 6.876*** |
| | (0.044) | (0.071) | | (0.043) | (0.028) | |
| Gas | –0.131** | 0.001 | 6.596** | –0.178*** | –0.071** | 13.556*** |
| | (0.052) | (0.085) | | (0.052) | (0.033) | |
| Gold | 0.171*** | 0.184*** | 0.208 | 0.107*** | 0.087*** | 3.159* |
| | (0.032) | (0.052) | | (0.020) | (0.013) | |
| Copper | 0.054 | 0.169** | 7.308*** | 0.037 | 0.084*** | 6.560** |
| | (0.041) | (0.069) | | (0.033) | (0.021) | |
| Sugar | 0.287*** | 0.467*** | 10.052*** | 0.100* | 0.158*** | 3.314* |
| | (0.062) | (0.102) | | (0.057) | (0.037) | |
| Wheat | –0.091** | –0.168** | 3.786* | 0.049 | 0.059*** | 0.274 |
| | (0.045) | (0.074) | | (0.035) | (0.023) | |

*Note.* This table reports estimates of the long-run multipliers $\beta^+$ and $\beta^-$ corresponding to Equation (5), based on the single-step estimation approach of Shin et al. (2014) and the two-step approach of Cho et al. (2020). For the former, we follow the general-to-specific procedure described in Table 2. Furthermore, the Wald statistic $\mathcal{W}_l$ for the test of long-run symmetry ($H_0 : \beta^+ = \beta^-$) is presented, with significance based on asymptotic $p$-values. Note that in the one-step framework the multipliers $\beta^+$ and $\beta^-$ are given by $-\theta^+/\rho$ and $-\theta^-/\rho$, respectively, and in the two-step framework by $\lambda + \eta$ and $\eta$. Standard errors are reported in parentheses, computed using the Delta method—except for the standard error of the estimate of $\beta^-$ in the two-step framework, which is obtained directly. *, **, and *** indicate significance at a 10%, 5%, and 1% significance level, respectively.

copper and sugar we conclude that the long-run price reaction to a decrease in uncertainty is stronger than to an increase, meaning that predominantly negative CPU shocks result in long-lasting (negative) changes in copper and sugar prices. Lastly, for wheat the Wald test statistic indicates that the long-run multipliers are not significantly different from each other, suggesting that long-run symmetry may be imposed. This would reduce the number parameters to be estimated and could improve estimation precision, which is particularly useful in small samples (Shin et al., 2014). However, Shin et al. (2014) also emphasize that invalid symmetry restrictions could cause serious model mis-specification. As the results in the table provide some evidence of asymmetry for wheat and given the size of our sample, we therefore do not specify such a restriction in subsequent steps of our analysis. Overall, the results demonstrate the importance of accounting for asymmetries in the relationship between global CPU and the commodity prices, justifying the nonlinear ARDL approach.

## 4.2 Short-Run Dynamics

Next, we focus on the short-run dynamics between the commodity prices and the independent variables, conditional on the long-run equilibrium relationships. To this end, we estimate the model specified in Equation (8), comprising the second step of the two-step NARDL approach. Here, the error correction term $\varepsilon_t$ for each commodity is given by the residuals of the associated long-run equilibrium relationship.

Table 4: Dynamic Coefficient Estimates Two-Step NARDL

| Oil | | | Gas | | | Gold | | | Copper | | | Sugar | | | Wheat | | |
|---|---|---|---|---|---|---|---|---|---|---|---|---|---|---|---|---|---|
| Var. | Coeff. | S.E. | Var. | Coeff. | S.E. | Var. | Coeff. | S.E. | Var. | Coeff. | S.E. | Var. | Coeff. | S.E. | Var. | Coeff. | S.E. |
| Const. | −0.04 | 0.01 | Const. | 0.01 | 0.01 | Const. | 0.02 | 0.00 | Const. | 0.01 | 0.01 | Const. | 0.02 | 0.01 | Const. | 0.02 | 0.01 |
| $\text{ECT}_{t-1}$ | −0.16 | 0.03 | $\text{ECT}_{t-1}$ | −0.19 | 0.03 | $\text{ECT}_{t-1}$ | −0.17 | 0.03 | $\text{ECT}_{t-1}$ | −0.13 | 0.03 | $\text{ECT}_{t-1}$ | −0.12 | 0.03 | $\text{ECT}_{t-1}$ | −0.17 | 0.03 |
| $\Delta y_{t-1}$ | −0.12 | 0.05 | $\Delta y_{t-9}$ | −0.13 | 0.05 | $\Delta y_{t-1}$ | −0.17 | 0.05 | $\Delta y_{t-5}$ | 0.15 | 0.05 | $\Delta y_{t-2}$ | 0.14 | 0.05 | $\Delta y_{t-5}$ | 0.12 | 0.05 |
| $\Delta y_{t-4}$ | −0.11 | 0.05 | $\Delta u^{-}_{t-12}$ | 0.16 | 0.07 | | | | $\Delta y_{t-11}$ | 0.13 | 0.05 | $\Delta u^{+}_{t}$ | 0.09 | 0.04 | $\Delta u^{+}_{t-2}$ | −0.06 | 0.03 |
| $\Delta y_{t-5}$ | 0.15 | 0.05 | | | | | | | $\Delta u^{-}_{t-9}$ | −0.07 | 0.04 | $\Delta u^{+}_{t-5}$ | −0.10 | 0.04 | $\Delta u^{+}_{t-8}$ | 0.19 | 0.04 |
| $\Delta y_{t-10}$ | 0.11 | 0.05 | | | | | | | | | | $\Delta u^{-}_{t-12}$ | 0.14 | 0.05 | $\Delta u^{-}_{t-5}$ | 0.09 | 0.04 |
| $\Delta u^{+}_{t-1}$ | 0.09 | 0.04 | | | | | | | | | | | | | $\Delta u^{-}_{t-7}$ | 0.16 | 0.05 |
| $\Delta u^{+}_{t-2}$ | −0.09 | 0.04 | | | | | | | | | | | | | $\Delta u^{-}_{t-10}$ | 0.11 | 0.04 |
| $\Delta u^{+}_{t-4}$ | −0.14 | 0.04 | | | | | | | | | | | | | | | |
| $\Delta u^{+}_{t-8}$ | −0.10 | 0.04 | | | | | | | | | | | | | | | |
| $\Delta u^{-}_{t-1}$ | −0.16 | 0.06 | | | | | | | | | | | | | | | |
| $\Delta u^{-}_{t-3}$ | −0.16 | 0.05 | | | | | | | | | | | | | | | |
| Adj. $R^2$ | 0.50 | | | 0.25 | | | 0.35 | | | 0.38 | | | 0.26 | | | 0.32 | |
| $\chi^2_{SC}$ | 7.92 [0.79] | | | 11.88 [0.46] | | | 24.00 [0.02] | | | 10.83 [0.54] | | | 8.61 [0.74] | | | 17.02 [0.15] | |
| $\chi^2_{HET}$ | 20.76 [0.19] | | | 12.32 [0.34] | | | 10.99 [0.44] | | | 12.87 [0.38] | | | 15.72 [0.33] | | | 23.62 [0.21] | |
| $\chi^2_{FF}$ | 5.24 [0.07] | | | 0.63 [0.73] | | | 4.81 [0.09] | | | 4.45 [0.11] | | | 1.04 [0.59] | | | 0.31 [0.86] | |
| $\chi^2_{NOR}$ | 17.98 [0.00] | | | 1.38 [0.50] | | | 30.87 [0.00] | | | 13.56 [0.00] | | | 1.84 [0.40] | | | 23.65 [0.00] | |
| CUSUM | Stable | | | Stable | | | Stable | | | Stable | | | Stable | | | Stable | |
| CUSUMSQ | Stable | | | Stable | | | Stable | | | Stable | | | Stable | | | Stable | |
| $\mathcal{W}_s$ | 1.79 [0.18] | | | 5.35 [0.02] | | | NA | | | 3.75 [0.05] | | | 4.49 [0.03] | | | 9.67 [0.00] | |

*Note.* This table reports estimation results of the NARDL model specified in Equation (8), corresponding to the second step of the two-step estimation approach of Cho et al. (2020). A general-to-specific procedure is used to arrive at the final NARDL model specification. Here, we set the maximum lag order equal to 12 and sequentially drop the insignificant dynamic regressors, with a 5% unidirectional decision rule. ECT is the error correction term associated with the long-run relationship estimated in the first step and $\chi^2_{SC}$, $\chi^2_{HET}$, $\chi^2_{FF}$, and $\chi^2_{NOR}$ denote the LM tests for serial correlation (Breusch-Godfrey), heteroskedasticity (Breusch-Pagan), functional form (Ramsey's RESET), and normality (Jarque-Bera), respectively. Furthermore, CUSUM(SQ) denotes the test for stability of the regression coefficients and $\mathcal{W}_s$ is the Wald statistic for the test of short-run additive symmetry ($H_0 : \sum_{j=0}^{q-1} \pi_j^+ = \sum_{j=0}^{q-1} \pi_j^-$). Asymptotic $p$-values are reported in brackets for all tests. Lastly, in order to conserve space we do not present the coefficient estimates for the set of control variables.

The dynamic estimation results obtained in the second step are presented in Table 4. For comparative purposes, the one-step NARDL results are given in Appendix D. To conserve space, the coefficient estimates for the set of control variables are not reported. First, we find that the preferred model specification varies considerably across the six commodities. For instance, in the NARDL model for oil numerous lags of $\Delta u_t^+$ and $\Delta u_t^-$ are significant, implying rich adjustment dynamics, while for gold no such short-run components are included. These differences highlight the relevance of our flexible general-to-specific modeling strategy. Furthermore, we see that the estimated coefficients of the error correction terms are close to each other, ranging from -0.12 for sugar to -0.19 for natural gas. These speed-of-adjustment parameters indicate at which rate the dependent variable converges towards the long-run equilibrium after a change in the exogenous variables (Engle and Granger, 1987; Granger, 1986). Importantly, since the parameters are between -1 and 0, we can conclude that for each commodity the equilibrium is stable (Banerjee et al., 1998; Westerlund, 2007). Depending on the commodity, a (permanent) deviation of global CPU from the trend in one period is adjusted by around 12% to 19% per month in subsequent periods. The time it takes to correct 50% of this deviation—that is, the half-life—is then approximately 4 to 6 months.[11] Compared to the results of Greenwood-Nimmo and Shin (2013), who study the response of petroleum spot prices to changes in the price of crude oil and find adjustments toward equilibrium of 29-37% per month, this correction is somewhat slow. On the other hand, relating the real futures price of oil to a set of economic factors, He et al. (2010) find half-life values close to ours. Moreover, Abid (2020) reports similar speed-of-adjustment parameters in his study on the relation between EPU on exchange rates. This discrepancy may be due to the distinct nature of economic shocks, to which agents are generally not accustomed such that it takes longer from them to believe a certain shock is permanent (Brunner et al., 1980). Lastly, we observe that for most commodities the contemporaneous price response to changes in uncertainty is zero. The only exception is sugar, for which the results suggest a direct positive reaction in price following an increase in CPU.

The diagnostic tests presented in the bottom half of Table 4 illustrate that the models are in general correctly specified. Particularly, at a 5% significance level we find no evidence of heteroskedasticity or misspecification of the functional form. Moreover, the cumulative sum and cumulative sum of squares test indicate stability of the regression coefficients. Finally, we can assess short-run asymmetries based on the Wald test for additive short-run symmetry and the selected lags of $\Delta u_t^+$ and $\Delta u_t^-$. For natural gas, copper, sugar, and wheat, the significance of $\mathcal{W}_s$ provides support for hypothesis of additive asymmetry. For crude oil, on the other hand, the null hypothesis of additive symmetry is not rejected. However, based on the included lags of $\Delta u_t^+$ and $\Delta u_t^-$ we can conclude that the pair-wise form of short-run symmetry suggested by Shin et al. (2014) would not hold. Consequently, the patterns of adjustment of the commodity prices following positive and negative changes in global CPU will likely differ. The exact patterns of dynamic adjustment—which depend on the combination of long-run coefficients, speed-of-adjustment parameter, and short-run dynamics—will be investigated in more detail later on.

[11] The half-life values are computed as $\ln(2)/\rho$.

Table 5: Toda-Yamamoto Test for Granger Causality

| Null hypothesis | Oil | Gas | Gold | Copper | Sugar | Wheat |
|---|---|---|---|---|---|---|
| $u^+ \not\rightarrow y$ | 15.123** | 1.536 | 1.828 | 1.974 | 3.075 | 4.022 |
| $u^- \not\rightarrow y$ | 8.363 | 0.941 | 3.355 | 0.307 | 2.573 | 4.129 |
| $y \not\rightarrow u^+$ | 1.785 | 3.410 | 4.791 | 5.481 | 1.537 | 7.712 |
| $y \not\rightarrow u^-$ | 3.747 | 5.569 | 6.111 | 2.878 | 3.536 | 6.068 |

*Note.* This table reports the statistic of the Granger causality test developed by Toda and Yamamoto (1995), similar to the asymmetric causality approach of Hatemi-J (2012). $a \not\rightarrow b$ indicates that variable $a$ does not Granger-cause variable $b$. The optimal lag order of the VAR model used in the test is determined based on the Akaike information criterion, and we increase the number of lags until serial correlation in the residuals is resolved. Given the results of the unit root tests presented in Table 1, $d_{max}$ is set to one. ** indicates significance at a 5% significance level.

## 4.3 Granger Causality

We have established that for each commodity there exists a cointegrating relationship among the variables, meaning that the system composed of the commodity price, the global climate policy uncertainty index, and the control variables converges to a long-run equilibrium over time. Yet, in order to make decisive statements about the impact of changes in uncertainty on prices, we now turn to a discussion on causality. As mentioned before, in a cointegrated bivariate system there must be causality in at least one direction (Engle and Granger, 1987). However, the cointegrating relations found in the Section 4.1 do not directly imply a causal link between either of the partial sum processes associated with the CPU factor and any of the commodity prices.

Table 5 displays results of the Toda and Yamamoto (1995) test for Granger causality. As before, we do not report results for the control variables, since these are not of primary interest. For natural gas, gold, copper, sugar, and wheat, no evidence of a causal relation between the price series and $u_t^+$ or $u_t^-$ is found. This means that while for these commodities the variables under study move together over time, changes in global climate policy uncertainty do not induce changes in the prices. Contrarily, the results for oil suggest that there is a unidirectional causality running from the partial sum process $u_t^+$ of positive changes in global CPU to the commodity price. That is, positive uncertainty shocks lead to (negative) changes in the oil futures prices. On the other hand, no such relationship is observed for decreases in uncertainty. Again, this discrepancy underscores the usefulness of the NARDL approach.

## 4.4 Dynamic Adjustment Patterns

Given the NARDL estimation results, we can visualize how each commodity price series adjusts over time to changes in global CPU. For this purpose, we compute the cumulative dynamic multiplier effects. As explained before, these dynamic multipliers depend on the combination of long-run and short-run coefficient, as well as the speed of adjustment.

The cumulative dynamic multipliers associated with a one percent increase and decrease in climate policy

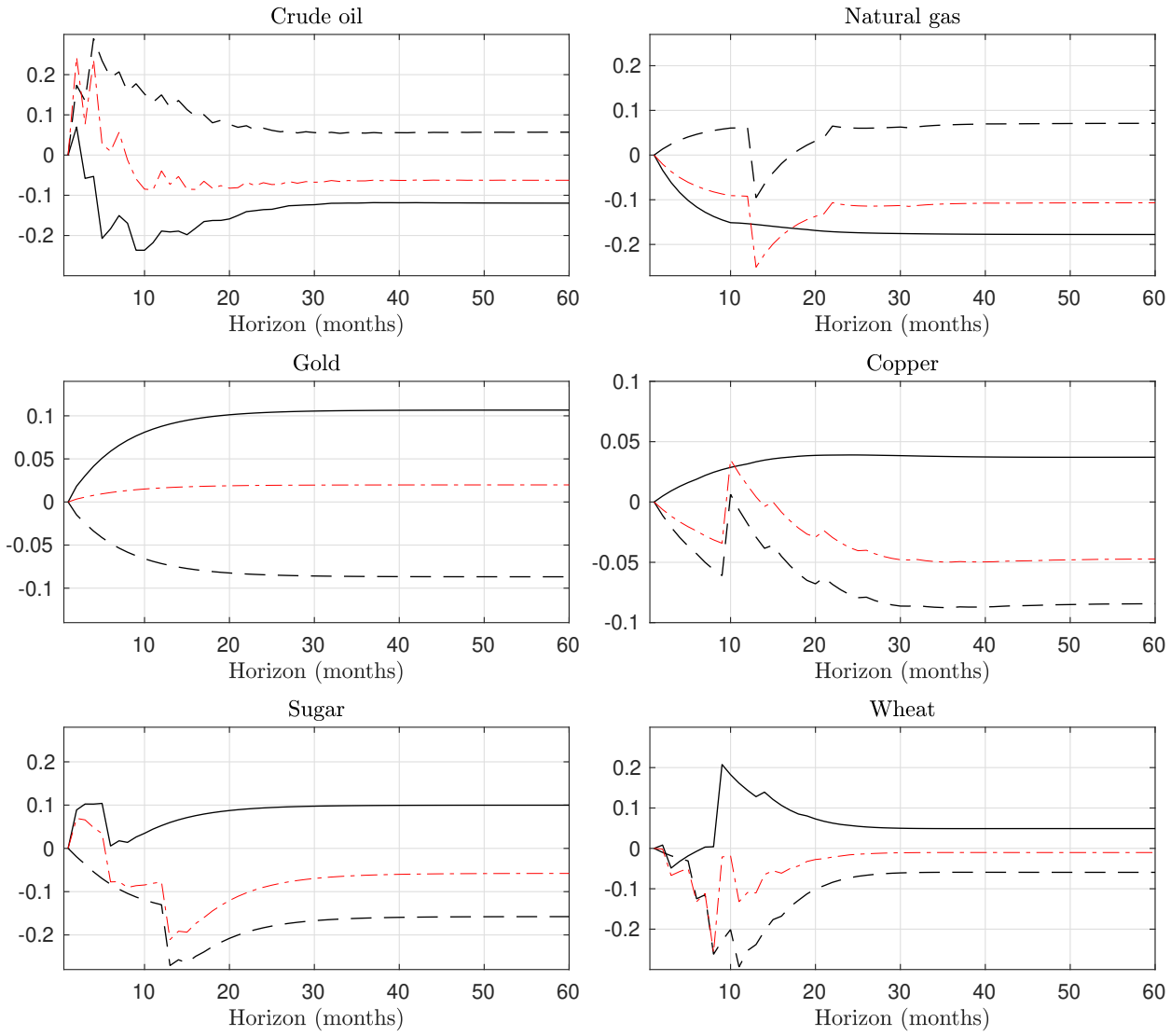


Figure 3: This figure plots the cumulative dynamic multipliers for each commodity based on the estimation results presented in Table 4. The solid and dashed black lines correspond to positive and negative changes in global climate policy uncertainty, respectively. The red line represents the asymmetry line.

uncertainty are plotted in Figure 3, corresponding to a shock of around 0.8 times the standard deviation of the CPU factor. First, the figure illustrates the rich adjustment dynamics across the six commodities, as well as the asymmetries in both the short-run and long-run. Note that the spikes, for instance apparent in the plots for natural gas, copper, and wheat, are due to the general-to-specific modeling approach which only selects significant lags. Of particular interest is the plot for crude oil, for which a causal link was found between uncertainty and the futures price. Following a positive shock in uncertainty, we initially observe a rather strong negative price reaction in the first ten months. In subsequent periods, the decline is partly offset. In the long run, a 1% increase in global CPU leads to a decrease in the (log) futures price of oil of around 0.12%, ceteris paribus. A 1% decrease in uncertainty is associated with only a 0.06% increase in the oil price in the

long run. Yet, both effects are statistically significant, as shown in Table 3. While no causality is found for the other commodities, the variables under study move together in a long-run equilibrium and the dynamic multipliers illustrate a clear relation between changes in uncertainty and changes in prices. Thereby, the results demonstrate the relevance of climate policy uncertainty as a risk factor underlying commodity markets.

From an investment perspective, this poses both threats and opportunities. For example, the observed asymmetry indicates that the response of futures prices to a positive CPU shock in one period need not be offset by a negative shock of equal magnitude in a subsequent period and vice versa. Consequently, participants in commodity futures markets need to be aware of the exposure of their commodity portfolio to this investment risk. In times of growing uncertainty about climate-related policy actions, the findings indicate that an allocation dominated by energy commodities may suffer considerably. On the other hand, in such times investors may protect their wealth by adequate diversification or focusing on other commodity classes like precious metals.

### 4.5 Economic Performance

Finally, we assess the economic implications of our empirical approach for investors by means of a forecasting exercise. More precisely, we investigate whether the two-step NARDL approach is able to produce more accurate commodity price forecasts than the benchmark models detailed in Section 3.4. The economic performance of all models is evaluated over the sub-sample from December 2016 to October 2020 (48 months). This period is especially interesting as it covers both large positive and negative changes in global CPU, as illustrated in Figure 2, such that it provides a useful testing environment for the NARDL models. The commodity price forecasts are constructed using an expanding estimation window as follows. First, given one of the commodities, we estimate each model over the period July 1996-November 2016 and compute dynamic one- to twelve-month-ahead forecasts. For the (nonlinear) ARDL models, in each iteration we adopt the general-to-specific approach described earlier. We then expand the estimation sample by one month and repeat the procedure, until the period corresponding to the twelve-month-ahead forecast is October 2020, which is the end of our sample. This way, we obtain 36 price forecasts for each horizon, model, and commodity.[12]

In Table 6 we present the root mean square percentage error (RMSPE) for the one- to twelve-month-ahead price forecasts produced by each of the competing models. Here, model NARDL-2S$^{\dagger}$ corresponds to the two-step NARDL approach where the global CPU factor is omitted. For each model and horizon, we have averaged the errors over the commodities, similar to an investor holding a portfolio of commodities. From the figures in the table, we can derive two key observations. First, the results indicate that the random walk benchmark outperforms the other models in the short run. This is in line with a substantial body of literature emphasizing that the RW model is a particularly tough competitor (see Fama, 1995; Rossi, 2013,

[12]Note that we study settlement prices of nearest commodity futures contracts. In practice, it will thus not be possible to hold one particular contract for more than a few months, as they expire. While such considerations are relevant when specifying an actual trading strategy, the results presented in this section are intended to serve an illustrative purpose.

Table 6: One- to Twelve-Month-Ahead Forecast Accuracy

| Model | 1 | 2 | 3 | 4 | 5 | 6 | 7 | 8 | 9 | 10 | 11 | 12 |
|---|---|---|---|---|---|---|---|---|---|---|---|---|
| ARDL | 4.58 | 5.95 | 7.50 | 8.52 | 9.37 | 10.25 | 11.16 | 11.56 | 11.99 | 12.20 | 12.73 | 13.18 |
| NARDL-1S | 4.71 | 5.98 | 7.01 | 7.66 | 8.38 | 9.12 | 9.95 | 10.45 | 10.69 | 10.35 | 11.29 | 11.77 |
| NARDL-2S | 4.42 | 5.58 | 6.67 | 7.32 | 8.16 | **8.77** | **9.02** | **9.25** | **9.72** | **9.62** | **10.10** | **10.49** |
| NARDL-2S$^{\dagger}$ | 4.31 | 5.79 | 7.44 | 8.45 | 9.63 | 11.08 | 12.26 | 13.05 | 13.98 | 14.73 | 15.64 | 16.36 |
| RW | **4.28** | **4.96** | **6.54** | **6.77** | **8.03** | 9.58 | 11.29 | 11.61 | 12.39 | 12.25 | 12.87 | 13.50 |

*Note.* This table reports the root mean square percentage error (RMSPE, %) for the one- to twelve-month-ahead ex-post out-of-sample commodity price forecasts produced by the ARDL model, one-step NARDL (NARDL-1S) approach, two-step NARDL (NARDL-2S) approach, and the random walk (RW) model with drift. Model NARDL-2S$^{\dagger}$ corresponds to the two-step NARDL approach where the global CPU factor is omitted. The presented figures are averages across the six primary commodities, with figures in bold indicating the minimum RMSPE at each horizon. Given one of the commodities, we estimate each model over the period 1996:7-2016:11 and compute dynamic one- to twelve-month-ahead forecasts. We then expand the estimation sample by one month and repeat the procedure, until the period corresponding to the twelve-month-ahead forecast is October 2020, which is the end of our sample. This yields 36 forecasts for each horizon, model, and commodity.

e.g.). Second, in the longer term we find that the two-step NARDL procedure yields, on average, the most accurate forecasts, achieving the lowest RMSPE at horizons of six months or more. While this seems to support the notion that adequate modeling of the long-run equilibrium in cointegrated systems improves forecasting power, for instance demonstrated by Zeng and Swanson (1998) in the context of commodity futures prices, the forecast accuracy deteriorates substantially in case the CPU factor is either omitted from the model or assumed to have a symmetric impact. Furthermore, there is a slight decline in performance when moving from the two-step to the one-step NARDL approach, which may be due to the fact that the parameter estimates obtained in the two-step framework are generally more precise, as we have seen before.

Altogether, the results presented in this empirical analysis highlight the relevance of climate policy uncertainty as a source of investment risk in global commodity markets. In particular, we demonstrate that commodity futures prices and global CPU move together in a stable equilibrium over time. Moreover, we establish that adequate modeling of their rich dynamic relation yields superior economic performance, especially in the longer run. From an investor's point of view, the results stress the importance of identification of climate-related risk factors, as well as knowledge regarding the exposure of individual commodities to these factors. Both components should be helpful for participants in commodity markets in terms of making portfolio decisions. At the same time, investors need to be alert to any potential regulatory changes, closely monitoring relevant political developments.

# 5 Conclusion

This paper investigates the dynamic relation between commodity prices and regulatory uncertainty associated with climate change. The main purpose of our study is to discern how changes in the global level of uncertainty affect the prices of primary commodities. To address this objective, we construct a novel global climate policy uncertainty index and specify a nonlinear autoregressive distributed lag model. This model allows us to simultaneously describe long-run cointegrating relations and short-run dynamics.

We apply our methodology to monthly futures prices on six primary commodities over the period 1996-2020 and illustrate the asymmetric nature of the relationship between commodity prices and climate policy uncertainty. For each commodity, we establish nonlinear cointegration between the price series, global CPU, and a set of economic controls, indicating that the variables converge towards a long-run equilibrium over time. Here, a deviation from the trend in one period is corrected by around 12% to 19% per month in subsequent periods. Combining these results with the short-run dynamics, rich patterns of price adjustment to uncertainty shocks are observed. With respect to causal links, we conclude that there is a unidirectional causality running from positive changes in global uncertainty to the price of crude oil. In the long run, an increase in CPU of 1% results in a decrease in the oil futures price of around 0.12%. Lastly, the forecast exercise highlights the economic benefit of our methodology, particularly in the medium to long term. Importantly, we present the first empirical application of the NARDL estimation procedure of Cho et al. (2020) and demonstrate its statistical value. The results suggest that we can improve the accuracy of commodity price forecasts when moving from the conventional one-step to the novel two-step framework.

In conclusion, our study accentuates the dynamic, asymmetric, and commodity-specific dependencies between commodity prices and climate-related regulatory uncertainty. Thereby, we emphasize the pertinence of this uncertainty as a source of investment risk in commodity markets. The implications of our findings for investors are twofold. First, commodity allocations may be hurt by unintended exposure to climate policy uncertainty. In light of the recent surges in uncertainty and given the strong negative association between CPU and the prices of oil and gas, this could be particularly the case when a portfolio is dominated by energy commodities. It is therefore suggested that participants in commodity markets carefully monitor climate-related political developments. Second, investors may exploit knowledge of the heterogeneous responses of commodity prices to uncertainty shocks, in order to hedge their overall position to changes in global CPU. For policymakers, of special significance is the evidence of a causal link from positive CPU shocks to the price of oil. While more research is needed to unravel the exact mechanisms through which higher global CPU leads to lower futures prices of oil—perhaps simply by affecting the decision-making process of speculators—the results indicate that investors and financial institutions may benefit from efforts to control policy uncertainty. Prompt resolution of climate-related policy issues should thus help safeguard financial stability.

# 6 Discussion

The current study presents several limitations that should be acknowledged, while it also opens up potential avenues for future research. First, in the construction of the global CPU index, we assume that the global level of uncertainty is given by the common factor of four country-level indexes. Although the set of countries includes the most influential nations, a sample of four is limited. Extending the analysis to additional countries may make the factor more reflective of worldwide uncertainty. However, this inevitably requires content analysis of non-English-language newspaper articles, making the selection of relevant (climate) search terms considerably more challenging. If this problem can be overcome, it would be interesting to construct CPU indexes for the other members of the G20, for example, as done by Baker et al. (2016) for their EPU indexes.

Second, in our analysis we have examined global CPU as a risk factor underlying commodity markets. Yet, a principal task in asset pricing is distinguishing redundant factors—i.e., factors whose variation can be explained by other risk factors—from those that actually price assets. Existing literature provides evidence that the EPU indexes of Baker et al. (2016) are in fact priced risk factors. For instance, Brogaard and Detzel (2015) establish that exposure to U.S. EPU is priced in the cross-section of U.S. stock returns. From an explanatory point of view, a useful direction for further research would thus be to assess whether CPU is a priced risk factor in commodity (futures) markets, or whether it is spanned by other factors.

Third, in this study we have used settlement prices of nearest futures contracts on six primary commodities. Generally, these contracts have a time to maturity of only a few weeks, which has various implications with respect to portfolio management. Specifically, contrary to the assumption implicitly made in our forecast exercise, holding one particular contract for several months is not possible. One might therefore argue that this exercise does not evaluate the true economic merit of our methodology, but rather the statistical benefit. Accordingly, future studies could build on our work by exploiting the findings to implement commodity trading strategies, while taking into account the peculiarities of commodity futures markets. For example, one could employ various methods such as the difference- or ratio-adjusted technique to determine rolling futures prices (Hamilton and Wu, 2015). Since trading is not our main focus, this is beyond the scope of this study.

Finally, we should note that in parallel with our research, Nam (2021) conducted a study that is connected to this paper. In particular, Nam (2021) investigates the impact of extreme climate events on global commodity spot markets by analyzing fluctuations in the El Niño–Southern Oscillation. These fluctuations represent a form of climate uncertainty and often trigger weather events such as droughts and hurricanes, thereby impacting physical assets and commodities. While the article would be an interesting reference, both for the literature review and empirical analysis, it was only just published in the latest issue of Energy Economics. For this reason, it is not discussed in our main text. Nevertheless, given the focus of Nam's (2021) study, our contributions to the literature remain unaltered.

# References

Abid, A. (2020). Economic policy uncertainty and exchange rates in emerging markets: Short and long runs evidence. *Finance Research Letters*, 37:101378.

Ahir, H., Bloom, N., and Furceri, D. (2018). The world uncertainty index. Stanford mimeo.

Ahumada, H. and Cornejo, M. (2015). Explaining commodity prices by a cointegrated time series-cross section model. *Empirical Economics*, 48(4):1667–1690.

Arango, L. E., Arias, F., and Flórez, A. (2011). Determinants of commodity prices. *Applied Economics*, 44(2):135–145.

Bahmani-Oskooee, M., Huynh, T. L. D., and Nasir, M. A. (2020). On the asymmetric effects of exchange-rate volatility on trade flows: Evidence from US–UK commodity trade. *Scottish Journal of Political Economy*, 68(1):51–102.

Bai, J. and Wang, P. (2015). Identification and Bayesian estimation of dynamic factor models. *Journal of Business & Economic Statistics*, 33(2):221–240.

Baker, S. R., Bloom, N., and Davis, S. J. (2016). Measuring economic policy uncertainty. *The Quarterly Journal of Economics*, 131(4):1593–1636.

Baker, S. R., Bloom, N., Davis, S. J., and Terry, S. J. (2020). COVID-induced economic uncertainty. Working paper, National Bureau of Economic Research.

Banerjee, A., Dolado, J., and Mestre, R. (1998). Error-correction mechanism tests for cointegration in a single-equation framework. *Journal of Time Series Analysis*, 19(3):267–283.

Bårdsen, G. (1989). Estimation of long run coefficients in error correction models. *Oxford Bulletin of Economics and Statistics*, 51(3):345–350.

Baur, D. G. and Lucey, B. M. (2010). Is gold a hedge or a safe haven? An analysis of stocks, bonds and gold. *Financial Review*, 45(2):217–229.

Belke, A., Bordon, I. G., and Hendricks, T. W. (2010). Global liquidity and commodity prices—A cointegrated VAR approach for OECD countries. *Applied Financial Economics*, 20(3):227–242.

Berger, T., Grabert, S., and Kempa, B. (2017). Global macroeconomic uncertainty. *Journal of Macroeconomics*, 53:42–56.

Bilgin, M. H., Gozgor, G., Lau, C. K. M., and Sheng, X. (2018). The effects of uncertainty measures on the price of gold. *International Review of Financial Analysis*, 58:1–7.

Boykoff, M. T. and Rajan, S. R. (2007). Signals and noise: Mass-media coverage of climate change in the USA and the UK. *EMBO Reports*, 8(3):207–211.

Breitenfellner, A. and Cuaresma, J. C. (2008). Crude oil prices and the USD/EUR exchange rate. *Monetary Policy & the Economy*, 4:102–121.

Brogaard, J. and Detzel, A. (2015). The asset-pricing implications of government economic policy uncertainty. *Management Science*, 61(1):3–18.

Brunner, A. D. (2002). El Niño and world primary commodity prices: Warm water or hot air? *Review of Economics and Statistics*, 84(1):176–183.

Brunner, K., Cukierman, A., and Meltzer, A. H. (1980). Stagflation, persistent unemployment and the permanence of economic shocks. *Journal of Monetary Economics*, 6(4):467–492.

Caldecott, B., Harnett, E., Cojoianu, T., Kok, I., and Pfeiffer, A. (2016). Stranded assets: A climate risk challenge. *Washington DC: Inter-American Development Bank*.

Chen, N.-F., Roll, R., and Ross, S. A. (1986). Economic forces and the stock market. *Journal of Business*, pages 383–403.

Cho, J. S., Greenwood-Nimmo, M., Shin, Y., et al. (2020). Two-step estimation of the nonlinear autoregressive distributed lag model. Working paper, Yonsei Economics Research Institute.

Coleman, L. (2012). Explaining crude oil prices using fundamental measures. *Energy Policy*, 40:318–324.

Deaton, A. and Laroque, G. (1992). On the behaviour of commodity prices. *The Review of Economic Studies*, 59(1):1–23.

Dempster, A. P., Laird, N. M., and Rubin, D. B. (1977). Maximum likelihood from incomplete data via the EM algorithm. *Journal of the Royal Statistical Society: Series B*, 39(1):1–22.

Dickey, D. A. and Fuller, W. A. (1981). Likelihood ratio statistics for autoregressive time series with a unit root. *Econometrica*, pages 1057–1072.

Diffenbaugh, N. S., Hertel, T. W., Scherer, M., and Verma, M. (2012). Response of corn markets to climate volatility under alternative energy futures. *Nature Climate Change*, 2(7):514–518.

Drachal, K. (2016). Forecasting spot oil price in a dynamic model averaging framework—Have the determinants changed over time? *Energy Economics*, 60:35–46.

Duasa, J. (2007). Determinants of Malaysian trade balance: An ARDL bound testing approach. *Global Economic Review*, 36(1):89–102.

Dwyer, A., Gardner, G., Williams, T., et al. (2011). Global commodity markets—Price volatility and financialisation. *RBA Bulletin*, pages 49–57.

Engle, R. F., Giglio, S., Kelly, B., Lee, H., and Stroebel, J. (2020). Hedging climate change news. *The Review of Financial Studies*, 33(3):1184–1216.

Engle, R. F. and Granger, C. W. (1987). Co-integration and error correction: Representation, estimation, and testing. *Econometrica*, pages 251–276.

Erten, B. and Ocampo, J. A. (2013). Super cycles of commodity prices since the mid-nineteenth century. *World Development*, 44:14–30.

Fama, E. F. (1995). Random walks in stock market prices. *Financial Analysts Journal*, 51(1):75–80.

Fama, E. F. and French, K. R. (2016). Commodity futures prices: Some evidence on forecast power, premiums, and the theory of storage. In *The World Scientific Handbook of Futures Markets*, pages 79–102. World Scientific.

Frankel, J. A. (2006). The effect of monetary policy on real commodity prices. Technical report, National Bureau of Economic Research.

Fried, S., Novan, K., and Peterman, W. B. (2021). The macro effects of climate policy uncertainty. Working paper, ASSA Annual Meeting.

Fuss, S., Szolgayova, J., Obersteiner, M., and Gusti, M. (2008). Investment under market and climate policy uncertainty. *Applied Energy*, 85(8):708–721.

Gilbert, C. L. (1989). The impact of exchange rates and developing country debt on commodity prices. *The Economic Journal*, 99(397):773–784.

Gorton, G. and Rouwenhorst, K. G. (2006). Facts and fantasies about commodity futures. *Financial Analysts Journal*, 62(2):47–68.

Gospodinov, N. and Jamali, I. (2018). Monetary policy uncertainty, positions of traders and changes in commodity futures prices. *European Financial Management*, 24(2):239–260.

Granger, C. W. (1969). Investigating causal relations by econometric models and cross-spectral methods. *Econometrica*, pages 424–438.

Granger, C. W. and Yoon, G. (2002). Hidden cointegration. Working paper, University of California, Department of Economics.

Granger, C. W. J. (1986). Developments in the study of cointegrated economic variables. In *Oxford Bulletin of Economics and Statistics*. Citeseer.

Greenwood-Nimmo, M. and Shin, Y. (2013). Taxation and the asymmetric adjustment of selected retail energy prices in the UK. *Economics Letters*, 121(3):411–416.

Grier, K. B., Henry, Ó. T., Olekalns, N., and Shields, K. (2004). The asymmetric effects of uncertainty on inflation and output growth. *Journal of Applied Econometrics*, 19(5):551–565.

Hamilton, J. D. (1994). State-space models. *Handbook of Econometrics*, 4:3039–3080.

Hamilton, J. D. and Wu, J. C. (2015). Effects of index-fund investing on commodity futures prices. *International Economic Review*, 56(1):187–205.

Hatemi-J, A. (2012). Asymmetric causality tests with an application. *Empirical Economics*, 43(1):447–456.

He, Y., Wang, S., and Lai, K. K. (2010). Global economic activity and crude oil prices: A cointegration analysis. *Energy Economics*, 32(4):868–876.

Hendry, D. F. (1995). *Dynamic econometrics*. Oxford University Press on Demand.

Hoffman, D. L. and Rasche, R. H. (1996). Assessing forecast performance in a cointegrated system. *Journal of Applied Econometrics*, 11(5):495–517.

Huang, J., Li, Y., Zhang, H., and Chen, J. (2021). The effects of uncertainty measures on commodity prices from a time-varying perspective. *International Review of Economics & Finance*, 71:100–114.

IPCC (2007). *Climate Change 2007: Synthesis Report. Contribution of Working Groups I, II and III to the Fourth Assessment Report of the Intergovernmental Panel on Climate Change*. IPCC Geneva, Switzerland.

IPCC (2014). *Climate-Resilient Pathways: Adaptation, Mitigation, and Sustainable Development*. Cambridge University Press.

IPCC (2018). *Global Warming of 1.5°C. An IPCC Special Report on the impacts of global warming of 1.5°C above pre-industrial levels and related global greenhouse gas emission pathways, in the context of strengthening the global response to the threat of climate change, sustainable development, and efforts to eradicate poverty*. In Press.

Ivanov, V., Kilian, L., et al. (2001). *A practitioner's guide to lag-order selection for vector autoregressions*, volume 2685. Centre for Economic Policy Research London.

Johansen, S. (1988). Statistical analysis of cointegration vectors. *Journal of Economic Dynamics and Control*, 12(2-3):231–254.

Johansen, S. and Juselius, K. (1990). Maximum likelihood estimation and inference on cointegration—With applications to the demand for money. *Oxford Bulletin of Economics and Statistics*, 52(2):169–210.

Kang, W., de Gracia, F. P., and Ratti, R. A. (2019). The asymmetric response of gasoline prices to oil price shocks and policy uncertainty. *Energy Economics*, 77:66–79.

Kapetanios, G., Shin, Y., and Snell, A. (2006). Testing for cointegration in nonlinear smooth transition error correction models. *Econometric Theory*, pages 279–303.

Katrakilidis, C. and Trachanas, E. (2012). What drives housing price dynamics in Greece: New evidence from asymmetric ARDL cointegration. *Economic Modelling*, 29(4):1064–1069.

Kilian, L. (2009). Not all oil price shocks are alike: Disentangling demand and supply shocks in the crude oil market. *American Economic Review*, 99(3):1053–69.

Kilian, L. (2019). Measuring global real economic activity: Do recent critiques hold up to scrutiny? *Economics Letters*, 178:106–110.

Kilian, L. and Zhou, X. (2018). Modeling fluctuations in the global demand for commodities. *Journal of International Money and Finance*, 88:54–78.

Kose, M. A., Otrok, C., and Whiteman, C. H. (2003). International business cycles: World, region, and country-specific factors. *American Economic Review*, 93(4):1216–1239.

Kwiatkowski, D., Phillips, P. C., Schmidt, P., and Shin, Y. (1992). Testing the null hypothesis of stationarity against the alternative of a unit root: How sure are we that economic time series have a unit root? *Journal of Econometrics*, 54(1-3):159–178.

Leiserowitz, A., Maibach, E., Rosenthal, S., Kotcher, J., Bergquist, P., Ballew, M. T., Goldberg, M., and Gustafson, A. (2020). *Climate change in the American mind: November 2019*. New Haven, CT: Yale Project on Climate Change Communication.

Lin, B. and Bai, R. (2021). Oil prices and economic policy uncertainty: Evidence from global, oil importers, and exporters' perspective. *Research in International Business and Finance*, 56:101357.

Lintner, J. (1965). Security prices, risk, and maximal gains from diversification. *The Journal of Finance*, 20(4):587–615.

Lütkepohl, H. (2005). *New introduction to multiple time series analysis*. Springer Science & Business Media.

Meese, R. A. and Rogoff, K. (1983). Empirical exchange rate models of the seventies: Do they fit out of sample? *Journal of International Economics*, 14(1-2):3–24.

Nam, K. (2021). Investigating the effect of climate uncertainty on global commodity markets. *Energy Economics*, 96:105123.

Nazlioglu, S. and Soytas, U. (2012). Oil price, agricultural commodity prices, and the dollar: A panel cointegration and causality analysis. *Energy Economics*, 34(4):1098–1104.

Newey, W. K. and West, K. D. (1987). A simple, positive semi-definite, heteroskedasticity and autocorrelationconsistent covariance matrix. Technical report, National Bureau of Economic Research.

Newey, W. K. and West, K. D. (1994). Automatic lag selection in covariance matrix estimation. *The Review of Economic Studies*, 61(4):631–653.

Pástor, L. and Veronesi, P. (2012). Uncertainty about government policy and stock prices. *The Journal of Finance*, 67(4):1219–1264.

Perron, P. (1989). The great crash, the oil price shock, and the unit root hypothesis. *Econometrica*, pages 1361–1401.

Pesaran, M. H. (1997). The role of economic theory in modelling the long run. *The Economic Journal*, 107(440):178–191.

Pesaran, M. H. and Shin, Y. (1995). An autoregressive distributed lag modelling approach to cointegration analysis. In *Strom, S. (Ed.), Econometrics and Economic Theory in the Twentieth Century: The Ragnar Frisch Centennial Symposium*, pages 371–413. Cambridge University Press.

Pesaran, M. H., Shin, Y., and Smith, R. J. (2001). Bounds testing approaches to the analysis of level relationships. *Journal of Applied Econometrics*, 16(3):289–326.

Phillips, P. C. and Hansen, B. E. (1990). Statistical inference in instrumental variables regression with I(1) processes. *The Review of Economic Studies*, 57(1):99–125.

Phillips, P. C. and Perron, P. (1988). Testing for a unit root in time series regression. *Biometrika*, 75(2):335–346.

Psaradakis, Z., Sola, M., and Spagnolo, F. (2004). On Markov error-correction models, with an application to stock prices and dividends. *Journal of Applied Econometrics*, 19(1):69–88.

Reilly, J., Hohmann, N., and Kane, S. (1994). Climate change and agricultural trade: Who benefits, who loses? *Global Environmental Change*, 4(1):24–36.

Ross, S. A. (1976). The arbitrage theory of capital asset pricing. *Journal of Economic Theory*, 13(3):341–360.

Rossi, B. (2013). Exchange rate predictability. *Journal of Economic Literature*, 51(4):1063–1119.

Sam, C. Y., McNown, R., and Goh, S. K. (2019). An augmented autoregressive distributed lag bounds test for cointegration. *Economic Modelling*, 80:130–141.

Schwartz, E. and Smith, J. E. (2000). Short-term variations and long-term dynamics in commodity prices. *Management Science*, 46(7):893–911.

Schwarz, G. (1978). Estimating the dimension of a model. *The Annals of Statistics*, 6(2):461–464.

Sharpe, W. F. (1964). Capital asset prices: A theory of market equilibrium under conditions of risk. *The Journal of Finance*, 19(3):425–442.

Shi, X. and Shen, Y. (2021). Macroeconomic uncertainty and natural gas prices: Revisiting the Asian Premium. *Energy Economics*, 94:105081.

Shin, Y., Yu, B., and Greenwood-Nimmo, M. (2014). Modelling asymmetric cointegration and dynamic multipliers in a nonlinear ARDL framework. In *Festschrift in Honor of Peter Schmidt*, pages 281–314. Springer.

Shrestha, M. B. and Bhatta, G. R. (2018). Selecting appropriate methodological framework for time series data analysis. *The Journal of Finance and Data Science*, 4(2):71–89.

Sims, C. A. (1980). Macroeconomics and reality. *Econometrica*, pages 1–48.

Tan, X. and Ma, Y. (2017). The impact of macroeconomic uncertainty on international commodity prices. *China Finance Review International*.

Taylor, M. P. (1995). The economics of exchange rates. *Journal of Economic literature*, 33(1):13–47.

Thackeray, S., Robinson, S., Smith, P., Bruno, R., Kirschbaum, M., et al. (2020). Civil disobedience movements such as School Strike for the Climate are raising public awareness of the climate change emergency. *Global Change Biology*, 26(3):1042–1044.

Toda, H. Y. and Yamamoto, T. (1995). Statistical inference in vector autoregressions with possibly integrated processes. *Journal of Econometrics*, 66(1-2):225–250.

Westerlund, J. (2007). Testing for error correction in panel data. *Oxford Bulletin of Economics and statistics*, 69(6):709–748.

Wu, L. S.-Y., Pai, J. S., and Hosking, J. (1996). An algorithm for estimating parameters of state-space models. *Statistics & Probability Letters*, 28(2):99–106.

Yang, M., Blyth, W., Bradley, R., Bunn, D., Clarke, C., and Wilson, T. (2008). Evaluating the power investment options with uncertainty in climate policy. *Energy Economics*, 30(4):1933–1950.

You, W., Guo, Y., Zhu, H., and Tang, Y. (2017). Oil price shocks, economic policy uncertainty and industry stock returns in China: Asymmetric effects with quantile regression. *Energy Economics*, 68:1–18.

Zeng, T. and Swanson, N. R. (1998). Predictive evaluation of econometric forecasting models in commodity futures markets. *Studies in Nonlinear Dynamics & Econometrics*, 2(4).

Zivot, E. and Andrews, D. W. K. (2002). Further evidence on the Great Crash, the oil-price shock, and the unit-root hypothesis. *Journal of Business & Economic Statistics*, 20(1):25–44.

# Appendix A Construction of Climate Policy Uncertainty Indexes

As outlined in Section 2.1, to construct the CPU indexes for the United States, United Kingdom, Australia, and China we adopt the newspaper-based approach of Baker et al. (2016). We search the digital archives of various leading newspapers using the Factiva global news database. This database is particularly convenient, as it offers a wide range of newspapers and it allows us to filter all published newspaper articles through specific search queries, restricting search results by newspaper, month, and language, for instance. For an article to be counted as a CPU article, it should contain at least one term in all three EPU categories—the economy (E), policy (P), and uncertainty (U)—as well as a term in the climate (C) category.

All term sets are derived from Baker et al. (2016) and the EPU website, except for the C term set, which is inspired by the climate change vocabulary (CCV) of Engle et al. (2020). In particular, the E term set consists of "economy" and "economic," and the U term set of "uncertain," "uncertainty," and "uncertainties." For the C term set we use the terms from the CCV that are most directly related to climate change, namely "climate," "climate change," "carbon," "greenhouse," "emission," and "emissions." Here, we exclude expressions that involve the word "climate" that are not associated with climate change, such as "climate of uncertainty," "economic climate," or "investment climate." Based on a sensitivity analysis, we concluded that other, less frequent terms from the CCV such as "temperature" or "energy" were not sufficient to isolate CPU articles. The country-specific sets of policy terms are presented below. Besides, we specify the set of newspapers considered in the construction of each CPU index, chosen based on data availability. Unless stated otherwise, the articles for each newspaper are available over the whole sample period, i.e., from July 1996 to October 2020.

*United States*

For the United States, the P term set contains "Federal Reserve," "the Fed," "deficit," "deficits," "Congress," "congressional," "White House," "legislation," "legislative," "legislature," "regulation," "regulations," and "regulatory." The six American newspaper we use are USA Today, the New York Times, the Wall Street Journal, the Washington Post, the Chicago Daily Herald (available from November 1997), and the Boston Globe.

*United Kingdom*

For the United Kingdom, the P term set contains "Bank of England," "spending," "policy," "deficit," "budget," "tax," and "regulation." The five U.K. newspapers we use are the Times, the Financial Times, the Guardian, the Daily Telegraph (available from November 2000), and the Independent.

*Australia*

For Australia, the P term set contains "Reserve Bank of Australia," "RBA," "deficit," "tax," "taxation," "taxes," "Parliament," "Senate," "cash rate," "tariff," "war," "legislation," and "regulation." The five Australian newspapers we use are the Australian, the Australian Financial Review, the Sydney Morning Herald, the Age, and the Canberra Times (available from September 1996).

*China*

Lastly, for China we consider a compound filter to select policy-related articles, following Baker et al. (2016). Specifically, an article should contain "tax," "regulation," "regulatory," "central bank," "People's Bank of China," "PBOC," "deficit," or "WTO," or it should contain both "policy," "spending," "budget," "political," "interest rates," or "reform" and "government," "Beijing," or "authorities." Additionally, a Chinese CPU article should include the word "China" or "Chinese." The two Chinese newspapers we use are China Daily and the South China Morning Post.

# Appendix B Estimation of Dynamic Factor Model

To obtain smoothed estimates of the unobserved global uncertainty index, we write the dynamic factor model specified by Equations (1) and (2) in state-space representation as follows. Let $y_t$ be the $N \times 1$ vector of CPU realizations at time $t \in \{1, \ldots, T\}$, $\alpha$ the $N \times 1$ vector of constants, and $\xi_t$ the $K \times 1$ state vector collecting the realizations of the global factor and the country factors from time $t$ up to time $t-p+1$, where $p$ is the lag order of the VAR model for the latent factors and $K = (N+1)p$. Following the notation of Hamilton (1994), the measurement and state transition equation corresponding to the dynamic factor model are then given by

$$y_t = \alpha + H\xi_t + w_t, \tag{B.1}$$

$$\xi_t = F\xi_{t-1} + v_t, \tag{B.2}$$

with $\xi_t = (f_t^W, f_{1,t}, \ldots, f_{N,t}, \ldots, f_{t-p+1}^W, f_{1,t-p+1}, \ldots, f_{N,t-p+1})'$ and parameter matrices

$$H = \begin{bmatrix} H_1 & 0 \end{bmatrix}_{N \times K}, \quad H_1 = \begin{bmatrix} \beta_1 & \gamma_1 & & \\ \vdots & & \ddots & \\ \beta_N & & & \gamma_N \end{bmatrix}_{N \times (N+1)} \quad \text{and} \quad F = \begin{bmatrix} \Phi_1 & \cdots & \Phi_{p-1} & \Phi_p \\ I & & & \\ & \ddots & & \\ & & I & \end{bmatrix}_{K \times K}.$$

The elements of $w_t$ are assumed to be normally distributed with mean zero and diagonal covariance matrix $R$. Similarly, the first $N+1$ elements of $v_t$ are assumed to be normally distributed with mean zero and diagonal covariance matrix $Q$, while the remaining elements of $v_t$ are exactly zero. In order to achieve unique identification of this dynamic factor model, the first loading on the world factor and all loadings on the country factors are set to one, i.e., $\beta_1 = \gamma_1 = \ldots = \gamma_N = 1$ (see Bai and Wang, 2015).

## B.1 Kalman Filter and Smoother

We estimate the state vector $\xi_t$ along with its corresponding uncertainty using the Kalman filter and smoother (see Hamilton, 1994). Let $\hat{\xi}_{t|t} = E(\xi_t|\mathcal{I}_t)$ and $P_{t|t} = \text{var}(\xi_t|\mathcal{I}_t)$, with $\mathcal{I}_t = \{y_1, \ldots, y_t\}$ the information set up to time $t$. Given $\alpha$, $H$, $F$, $R$, and $Q$, the prediction step of the Kalman filter is specified as

$$\hat{\xi}_{t+1|t} = F\hat{\xi}_{t|t}, \tag{B.3}$$

$$P_{t+1|t} = FP_{t|t}F' + P'QP, \tag{B.4}$$

where $P = [I_{N+1}\ 0_{(N+1)\times(K-N-1)}]$, such that $P'QP$ is a $K \times K$ matrix with the top-left part equal to $Q$ and the other elements equal to zero. Next, we use the observed data $y_{t+1}$ to update our beliefs on the state vector according to the updating step of the Kalman filter:

$$\hat{\xi}_{t+1|t+1} = \hat{\xi}_{t+1|t} + P_{t+1|t}H'(HP_{t+1|t}H' + R)^{-1}(y_{t+1} - \alpha - H\hat{\xi}_{t+1|t}), \tag{B.5}$$

$$P_{t+1|t+1} = P_{t+1|t} - P_{t+1|t}H'(HP_{t+1|t}H' + R)^{-1}HP_{t+1|t}. \tag{B.6}$$

We loop through Equations (B.3) to (B.6) for $t = 0, \ldots, T-1$. Following Hamilton (1994), the filter is initialized by setting $\hat{\xi}_{1|0} = 0$, which is the unconditional expectation of $\xi_t$, and $P_{1|0} = I \times 10^6$.

Given the output of the Kalman filter, we iterate the Kalman smoothing equations backward in time:

$$\hat{\xi}_{t|T} = \hat{\xi}_{t|t} + P_{t|t}F'P^{-1}_{t+1|t}(\hat{\xi}_{t+1|T} - \hat{\xi}_{t+1|t}), \tag{B.7}$$

$$P_{t|T} = P_{t|t} - P_{t|t}F'P^{-1}_{t+1|t}(P_{t+1|t} - P_{t+1|T})P^{-1}_{t+1|t}FP_{t|t}, \tag{B.8}$$

$$P_{t+1,t|T} = P_{t+1|T}P^{-1}_{t+1|t}FP_{t|t}, \tag{B.9}$$

for $t = T, T-1, \ldots, 0$ and where $P_{t,t-1|T} = \text{cov}(\xi_t, \xi_{t-1}|\mathcal{I}_T)$.

## B.2 Expectation-Maximization Algorithm

To estimate the parameters of the dynamic factor model, the expectation-maximization (EM) algorithm of Dempster et al. (1977) is adopted. Compared to maximum likelihood estimation, EM tends to converge to a reasonable area of the parameter space relatively quickly. Moreover, a notable advantage of the EM algorithm over maximum likelihood is that it gets stuck less often in local optima.

In the first step of the algorithm (E-step), we run the Kalman filter and smoother conditional on some (initial) values of the model parameters, as outlined in Section B.1. In the second step (M-step), the output from the E-step is used to find analytical expressions for $\alpha$, $H$, $F$, $R$, and $Q$. The standard EM algorithm, however, does not account for restrictions on the elements of the system matrices $H$ and $F$. Therefore, inspired by Wu et al. (1996), the M-step is adjusted in two ways: the expression for $H$ is derived using a Lagrange multiplier approach and for $F$ we obtain an expression for the first $N+1$ rows, which are unrestricted.

First, we specify the joint density of the data $y_{1:T}$ and states $\xi_{0:T}$ as

$$\begin{aligned}\log L(y_{1:T}, \xi_{0:T}|\theta) \propto &-\frac{T}{2}\log|R| - \frac{1}{2}\sum_{t=1}^{T}(y_t - \alpha - H\xi_t)' R^{-1}(y_t - \alpha - H\xi_t) \\ &-\frac{T}{2}\log|Q| - \frac{1}{2}\sum_{t=1}^{T}(\xi_t - F\xi_{t-1})'P'Q^{-1}P(\xi_t - F\xi_{t-1}),\end{aligned} \tag{B.10}$$

where $\theta$ collects all parameters and a diffuse prior on $\xi_0$ is assumed. Next, we take the expectation of the log-likelihood conditional on the information set $\mathcal{I}_T$. Using the cyclic property of the trace, we can derive that

this conditional expectation is proportional to

$$\begin{aligned}
E(\log L|\mathcal{I}_T) \propto & -\frac{T}{2}\log|R| - \frac{1}{2}\sum_{t=1}^{T}\left(y_t - \alpha - H\hat{\xi}_{t|T}\right)' R^{-1}\left(y_t - \alpha - H\hat{\xi}_{t|T}\right) \\
& -\frac{T}{2}\log|Q| - \frac{1}{2}\sum_{t=1}^{T}\left(\hat{\xi}_{t|T} - F\hat{\xi}_{t-1|T}\right)' P'Q^{-1}P\left(\hat{\xi}_{t|T} - F\hat{\xi}_{t-1|T}\right) \\
\propto & -\frac{T}{2}\log|R| - \frac{1}{2}\mathrm{tr}\left\{R^{-1}\left(\sum_{t=1}^{T}(y_t-\alpha)(y_t-\alpha)' - DH' - HD' + HCH'\right)\right\} \\
& -\frac{T}{2}\log|Q| - \frac{1}{2}\mathrm{tr}\left\{P'Q^{-1}P(C - BF' - FB' + FAF')\right\}, \qquad \text{(B.11)}
\end{aligned}$$

where we have defined the matrices

$$\begin{aligned}
A &= \sum_{t=1}^{T}\left(\hat{\xi}_{t-1|T}\left(\hat{\xi}_{t-1|T}\right)' + P_{t-1|T}\right), \\
B &= \sum_{t=1}^{T}\left(\hat{\xi}_{t|T}\left(\hat{\xi}_{t-1|T}\right)' + P_{t,t-1|T}\right), \\
C &= \sum_{t=1}^{T}\left(\hat{\xi}_{t|T}\left(\hat{\xi}_{t|T}\right)' + P_{t|T}\right), \\
D &= \sum_{t=1}^{T}(y_t - \alpha)\left(\hat{\xi}_{t|T}\right)'.
\end{aligned}$$

Given the expression in Equation (B.11), we maximize the conditional expectation of the log-likelihood with respect to $\alpha$, $H$, $F$, $R$, and $Q$ to obtain analytical solutions for these quantities.

In the first step of the M-step we update the intercept vector $\alpha$ according to the standard EM-solution

$$\alpha = \frac{1}{T}\sum_{t=1}^{T}\left(y_t - H\hat{\xi}_{t|T}\right), \qquad \text{(B.12)}$$

which is straightforwardly derived by optimizing Equation (B.11) with respect to $\alpha$.

Next, consider $H$, and suppose that the constraints on the elements of $H$ can be written as $G \cdot \mathrm{vec}(H) = g$, where $G$ selects the fixed elements of $\mathrm{vec}(H)$ and $g$ is a vector of zeros and ones. Collecting all terms in the likelihood function of Equation (B.11) involving $H$ and rewriting the expression in terms of $\mathrm{vec}(H)$ gives

$$\begin{aligned}
-\frac{1}{2}\mathrm{tr}\left\{R^{-1}\left(-DH' - HD' + HCH'\right)\right\} &= \frac{1}{2}\left[\mathrm{tr}\left(R^{-1}DH'\right) + \mathrm{tr}\left(R^{-1}HD'\right) - \mathrm{tr}\left(R^{-1}HCH'\right)\right] \\
&= \frac{1}{2}\left[\mathrm{vec}\left(R^{-1}D\right)'\mathrm{vec}(H) + \mathrm{vec}\left(R^{-1}D\right)'\mathrm{vec}(H) - \mathrm{vec}(HC)'\mathrm{vec}\left(R^{-1}H\right)\right] \\
&= \mathrm{vec}\left(R^{-1}D\right)'\mathrm{vec}(H) - \frac{1}{2}\mathrm{vec}(H)'\left(C \otimes R^{-1}\right)\mathrm{vec}(H),
\end{aligned}$$

using the properties of the trace. In order to maximize this expression with respect to $\mathrm{vec}(H)$, subject to the constraint $G \cdot \mathrm{vec}(H) = g$, we specify the Lagrangian function as

$$\mathcal{L}(\mathrm{vec}(H), \lambda) = \mathrm{vec}\left(R^{-1}D\right)'\mathrm{vec}(H) - \frac{1}{2}\mathrm{vec}(H)'\left(C \otimes R^{-1}\right)\mathrm{vec}(H) - (g - G \cdot \mathrm{vec}(H))'\lambda,$$

with $\lambda$ the vector of Lagrange multipliers. The corresponding optimality conditions are given by

$$\begin{aligned}
\frac{\partial \mathcal{L}(\text{vec}(H), \lambda)}{\partial \lambda} &= (g - G \cdot \text{vec}(H))' = 0, \\
\frac{\partial \mathcal{L}(\text{vec}(H), \lambda)}{\partial \text{vec}(H)} &= \text{vec}\left(R^{-1}D\right) - \left(C \otimes R^{-1}\right)\text{vec}(H) + G'\lambda \\
&= \left(C^{-1} \otimes R\right)\text{vec}\left(R^{-1}D\right) - \text{vec}(H) + \left(C^{-1} \otimes R\right)G'\lambda \\
&= G \cdot \text{vec}\left(DC^{-1}\right) - G \cdot \text{vec}(H) + G\left(C^{-1} \otimes R\right)G'\lambda \\
&= G \cdot \text{vec}\left(DC^{-1}\right) - g + G\left(C^{-1} \otimes R\right)G'\lambda = 0,
\end{aligned}$$

where in the last line we use that $G \cdot \text{vec}(H) = g$, which follows from the first condition. Solving the second equation for $\lambda$ yields $\lambda = (G(C^{-1} \otimes R)G')^{-1}\{g - G \cdot \text{vec}(DC^{-1})\}$, which we plug into the second line of the second condition to arrive at the solution

$$\text{vec}(H) = \text{vec}\left(DC^{-1}\right) + \left(C^{-1} \otimes R\right)G'\left(G\left(C^{-1} \otimes R\right)G'\right)^{-1}\left\{g - G \cdot \text{vec}\left(DC^{-1}\right)\right\}. \tag{B.13}$$

Here, the first term on the right-hand side of the equation corresponds to the unrestricted EM-solution.

Similarly, for $F$ we collect all terms in the likelihood function involving $F$ and rewrite the expression as

$$\begin{aligned}
-\frac{1}{2}\text{tr}\left\{P'Q^{-1}P(-BF' - FB' + FAF')\right\} &= \frac{1}{2}\text{tr}\{Q^{-1}(PBF'P' + PFB'P' - PFAF'P')\} \\
&= \frac{1}{2}\text{tr}\left\{Q^{-1}\left(\widetilde{B}\widetilde{F}' + \widetilde{F}\widetilde{B}' - \widetilde{F}A\widetilde{F}'\right)\right\} \\
&= \frac{1}{2}\left[\text{tr}\left(Q^{-1}\widetilde{B}\widetilde{F}'\right) + \text{tr}\left(Q^{-1}\widetilde{F}\widetilde{B}'\right) - \text{tr}\left(Q^{-1}\widetilde{F}A\widetilde{F}'\right)\right],
\end{aligned}$$

where $\widetilde{B} = PB$ and $\widetilde{F} = PF$, selecting the first $N + 1$ rows of both matrices. Taking the derivative of this expression with respect to $\widetilde{F}$ and setting it equal to zero yields the solution

$$\widetilde{F} = \widetilde{B}A^{-1}. \tag{B.14}$$

Lastly, we update the covariance matrices $Q$ and $F$ using the diagonal elements of the unrestricted matrices

$$Q = T^{-1}\left(PCP' - \widetilde{B}\widetilde{F}' - \widetilde{F}\widetilde{B}' + \widetilde{F}A\widetilde{F}'\right), \tag{B.15}$$

$$R = T^{-1}\left(\textstyle\sum_{t=1}^{T}(y_t - \alpha)(y_t - \alpha)' - DH' - HD' + HCH'\right), \tag{B.16}$$

which can be derived by maximization of the conditional expectation of the log-likelihood function as before.

Together with the Kalman equations of Section B.1, Equations (B.12) to (B.16) constitute one step of the EM algorithm. The total number of iterations is set to 1,000. In order to identify the global optimum, the algorithm is run multiple times using random starting values and we select the parameters that yield the highest log-likelihood. Finally, to facilitate estimation we set lag order $p = 1$. Importantly, most autocorrelation in the residuals $\hat{\varepsilon}_t^W, \hat{\varepsilon}_{1,t}, \ldots, \hat{\varepsilon}_{N,t}$, corresponding to Equation (2) of the dynamic factor model, is eliminated.

# Appendix C Overview Variables

## C.1 Commodities

Table C.1: Commodity Futures Contracts

| Commodity | Exchange | Contract size | Contract months |
|---|---|---|---|
| Light crude oil, WTI spot Cushing | NYMEX | 1,000 barrels | F-Z |
| Natural gas, Henry Hub | NYMEX | 10,000 MMBtu | F-Z |
| Gold, Handy & Harman | NYMEX | 100 troy ounces | G, J, M, Q, V, Z |
| High grade copper, cathode | NYMEX | 25,000 lbs | H, K, N, U, Z |
| Sugar #11 | ICE | 112,000 lbs | H, K, N, V |
| Wheat composite | CBOT | 5,000 bushels | H, K, N, U, Z |

*Note.* This table presents a description of the commodity futures contracts used in the analysis. For each contract, we provide the name of the commodity, the futures exchange on which it is traded, the size of the contract, and the delivery months. Here, NYMEX denotes New York Mercantile Exchange, ICE denotes Intercontinental Exchange, and CBOT denotes Chicago Board of Trade. The codes for the months are F=January, G=February, H=March, J=April, K=May, M=June, N=July, Q=August, U=September, V=October, X=November, and Z=December.

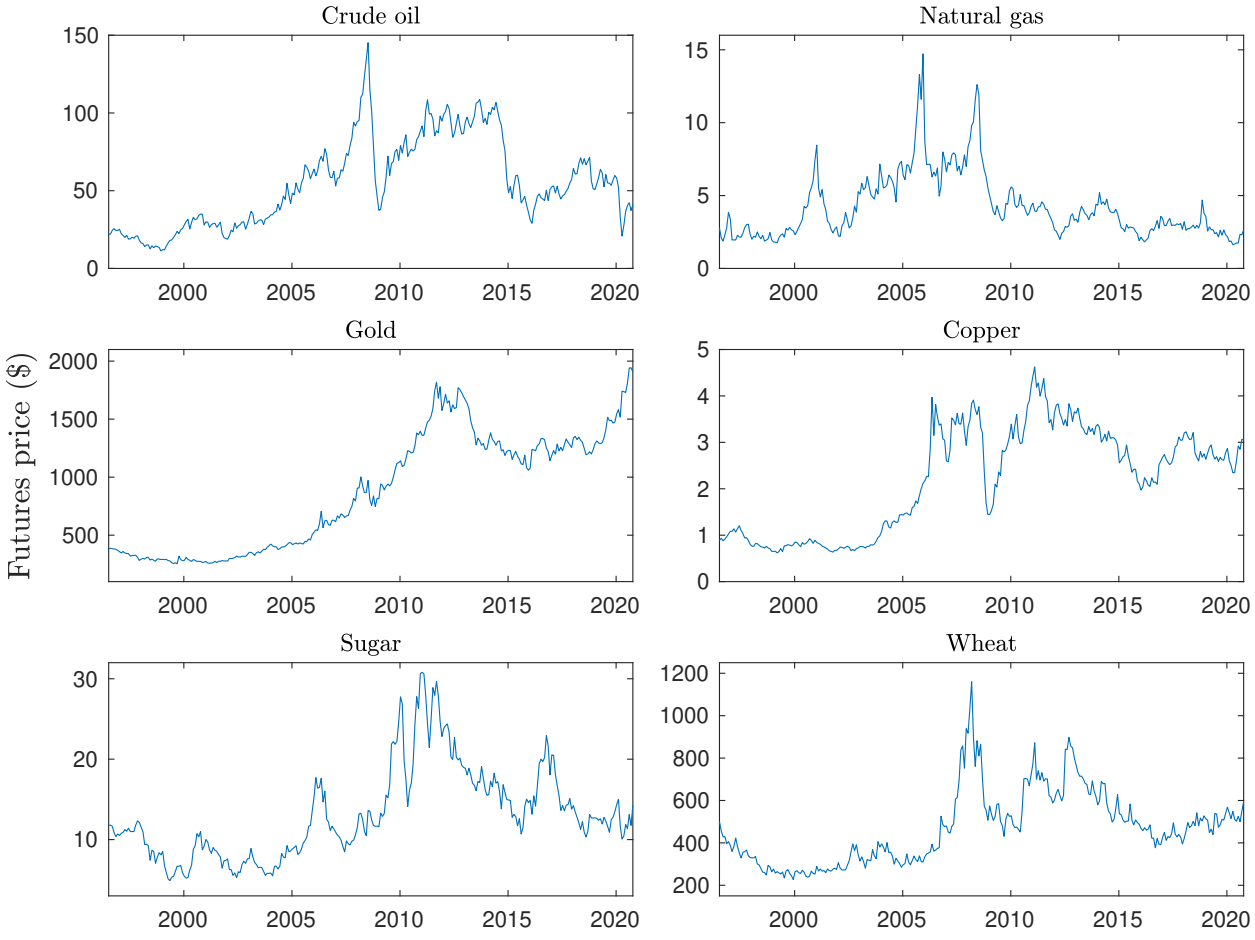


Figure 4: This figure plots the monthly settlement prices of nearest futures contracts on the six primary commodities considered in the empirical analysis over the period 1996:7-2020:10.

## C.2 Control Variables

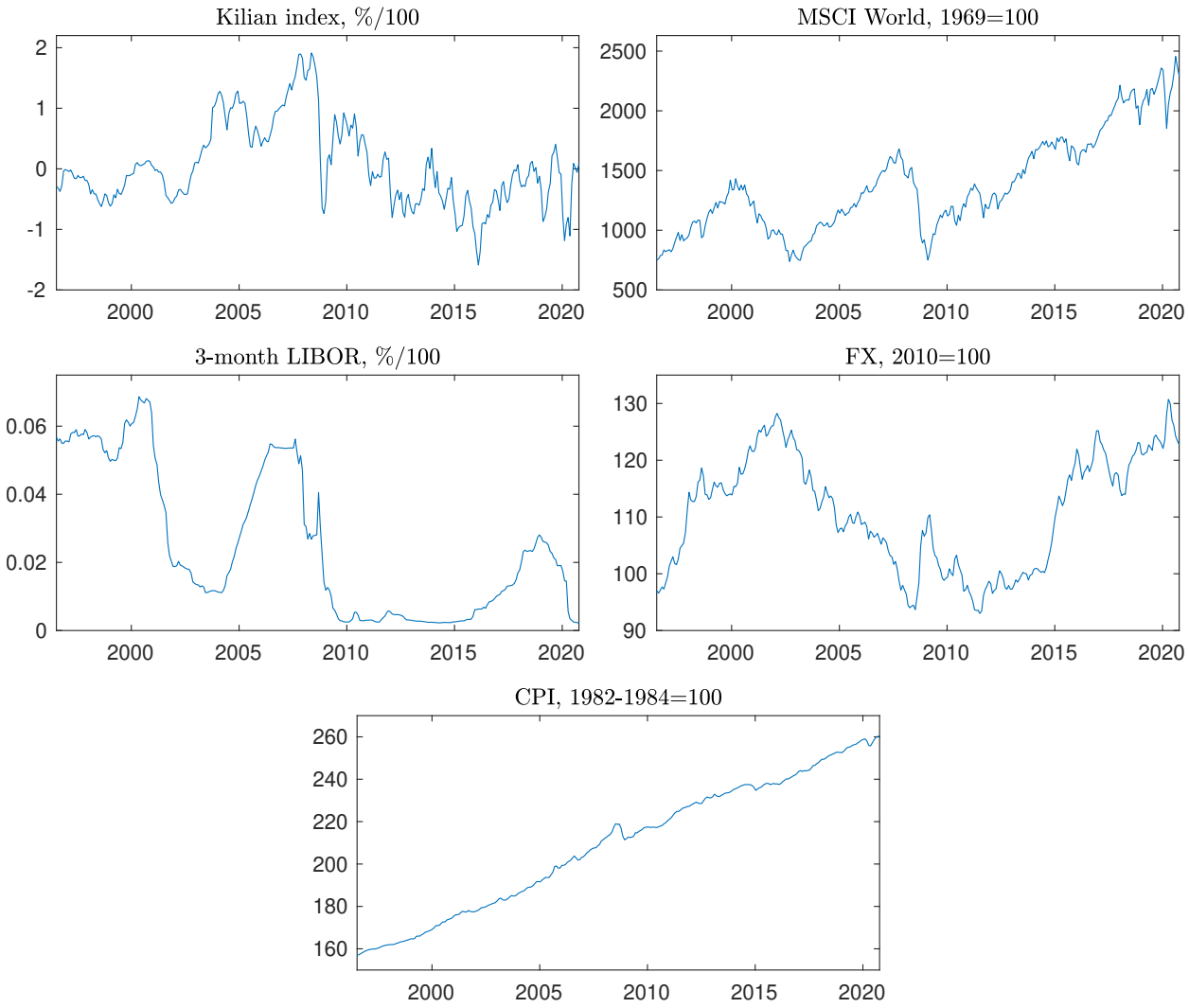


Figure 5: This figure plots the five control variables considered in the empirical analysis over the period 1996:7-2020:10. In particular, we employ Kilian's (2009) index of global real economic activity, the MSCI World stock market index, the 3-month London Interbank Offered Rate, the U.S. nominal effective exchange rate, and the U.S. consumer price index for all urban consumers.

## C.3 Descriptive Statistics

Table C.2: Descriptive Statistics

| Variable | Obs. | Mean | Median | Min. | Max. | Std. Dev. | Skew. | Kurt. |
|---|---|---|---|---|---|---|---|---|
| ln oil | 292 | 3.851 | 3.948 | 2.422 | 4.978 | 0.579 | –0.395 | 2.277 |
| ln gas | 292 | 1.325 | 1.276 | 0.490 | 2.689 | 0.465 | 0.479 | 2.570 |
| ln gold | 292 | 6.567 | 6.779 | 5.538 | 7.572 | 0.672 | –0.211 | 1.405 |
| ln copper | 292 | 0.621 | 0.924 | –0.480 | 1.531 | 0.627 | –0.456 | 1.598 |
| ln sugar | 292 | 2.485 | 2.468 | 1.589 | 3.428 | 0.425 | 0.036 | 2.425 |
| ln wheat | 292 | 6.089 | 6.122 | 5.425 | 7.056 | 0.357 | 0.151 | 2.221 |
| CPU | 292 | –0.129 | –0.512 | –1.630 | 3.597 | 1.261 | 1.033 | 3.471 |
| Kilian | 292 | 0.045 | –0.089 | –1.588 | 1.913 | 0.685 | 0.684 | 3.037 |
| ln MSCI | 292 | 7.186 | 7.176 | 6.604 | 7.806 | 0.294 | 0.102 | 2.185 |
| LIBOR | 292 | 0.025 | 0.018 | 0.002 | 0.069 | 0.022 | 0.545 | 1.764 |
| ln FX | 292 | 4.703 | 4.721 | 4.533 | 4.873 | 0.091 | –0.134 | 1.739 |
| ln CPI | 292 | 5.332 | 5.362 | 5.056 | 5.562 | 0.152 | –0.268 | 1.762 |

*Note.* This table reports descriptive statistics of the variables used in the empirical study over the period 1996:7-2020:10. 'ln' indicates that the respective variable is transformed to natural logarithms. Furthermore, the Kilian index is measured as percent deviation from trend, MSCI as price index (1969=100), LIBOR as percent, FX as index (2010=100), and CPI as price index (1982-1984=100).

# Appendix D Dynamic Coefficient Estimates One-Step NARDL

Table D.1: Dynamic Coefficient Estimates One-Step NARDL

| Oil | | | Gas | | | Gold | | | Copper | | | Sugar | | | Wheat | | |
|---|---|---|---|---|---|---|---|---|---|---|---|---|---|---|---|---|---|
| Var. | Coeff. | S.E. | Var. | Coeff. | S.E. | Var. | Coeff. | S.E. | Var. | Coeff. | S.E. | Var. | Coeff. | S.E. | Var. | Coeff. | S.E. |
| Const. | −4.99 | 1.56 | Const. | −7.31 | 2.53 | Const. | 0.28 | 0.75 | Const. | −3.74 | 1.16 | Const. | −2.44 | 1.55 | Const. | 3.13 | 1.36 |
| $y_{t-1}$ | −0.19 | 0.03 | $y_{t-1}$ | −0.22 | 0.03 | $y_{t-1}$ | −0.15 | 0.03 | $y_{t-1}$ | −0.14 | 0.02 | $y_{t-1}$ | −0.16 | 0.03 | $y_{t-1}$ | −0.19 | 0.03 |
| $u^+_{t-1}$ | −0.02 | 0.01 | $u^+_{t-1}$ | −0.03 | 0.01 | $u^+_{t-1}$ | 0.03 | 0.01 | $u^+_{t-1}$ | 0.01 | 0.01 | $u^+_{t-1}$ | 0.05 | 0.01 | $u^+_{t-1}$ | −0.02 | 0.01 |
| $u^-_{t-1}$ | 0.00 | 0.01 | $u^-_{t-1}$ | 0.00 | 0.02 | $u^-_{t-1}$ | 0.03 | 0.01 | $u^-_{t-1}$ | 0.02 | 0.01 | $u^-_{t-1}$ | 0.07 | 0.02 | $u^-_{t-1}$ | −0.03 | 0.01 |
| $\Delta y_{t-4}$ | −0.10 | 0.05 | $\Delta y_{t-9}$ | −0.13 | 0.05 | $\Delta y_{t-1}$ | −0.19 | 0.05 | $\Delta y_{t-5}$ | 0.15 | 0.05 | $\Delta u^+_t$ | 0.10 | 0.04 | $\Delta u^+_{t-8}$ | 0.21 | 0.04 |
| $\Delta y_{t-5}$ | 0.19 | 0.05 | $\Delta u^-_{t-12}$ | 0.16 | 0.07 | $\Delta u^+_{t-6}$ | −0.04 | 0.02 | $\Delta y_{t-11}$ | 0.13 | 0.05 | $\Delta u^+_{t-5}$ | −0.11 | 0.04 | $\Delta u^-_{t-7}$ | 0.20 | 0.05 |
| $\Delta y_{t-10}$ | 0.13 | 0.05 | | | | | | | $\Delta u^+_{t-2}$ | −0.06 | 0.03 | $\Delta u^+_{t-7}$ | −0.11 | 0.04 | $\Delta u^-_{t-10}$ | 0.11 | 0.04 |
| $\Delta y_{t-12}$ | 0.11 | 0.05 | | | | | | | $\Delta u^-_{t-1}$ | −0.09 | 0.04 | $\Delta u^-_{t-8}$ | −0.17 | 0.05 | | | |
| $\Delta u^+_{t-1}$ | 0.09 | 0.04 | | | | | | | $\Delta u^-_{t-9}$ | −0.09 | 0.04 | $\Delta u^-_{t-9}$ | −0.12 | 0.05 | | | |
| $\Delta u^+_{t-2}$ | −0.10 | 0.04 | | | | | | | | | | $\Delta u^-_{t-12}$ | 0.16 | 0.05 | | | |
| $\Delta u^+_{t-4}$ | −0.15 | 0.04 | | | | | | | | | | | | | | | |
| $\Delta u^+_{t-7}$ | −0.09 | 0.04 | | | | | | | | | | | | | | | |
| $\Delta u^+_{t-8}$ | −0.11 | 0.04 | | | | | | | | | | | | | | | |
| $\Delta u^-_{t-1}$ | −0.17 | 0.06 | | | | | | | | | | | | | | | |
| $\Delta u^-_{t-3}$ | −0.15 | 0.05 | | | | | | | | | | | | | | | |
| Adj. $R^2$ | 0.52 | | | 0.23 | | | 0.36 | | | 0.39 | | | 0.33 | | | 0.29 | |
| $\chi^2_{SC}$ | 12.47 [0.41] | | | 12.72 [0.39] | | | 3.35 [0.34] | | | 13.76 [0.32] | | | 6.57 [0.88] | | | 15.88 [0.20] | |
| $\chi^2_{HET}$ | 24.09 [0.63] | | | 23.49 [0.10] | | | 24.17 [0.19] | | | 46.62 [0.00] | | | 33.83 [0.33] | | | 38.56 [0.02] | |
| $\chi^2_{FF}$ | 4.49 [0.11] | | | 0.13 [0.94] | | | 2.13 [0.35] | | | 5.15 [0.08] | | | 0.02 [0.99] | | | 0.17 [0.92] | |
| $\chi^2_{NOR}$ | 19.08 [0.00] | | | 4.42 [0.11] | | | 62.15 [0.00] | | | 20.40 [0.00] | | | 0.72 [0.70] | | | 21.54 [0.00] | |
| CUSUM | Stable | | | Stable | | | Stable | | | Stable | | | Stable | | | Stable | |
| CUSUMSQ | Stable | | | Stable | | | Stable | | | Stable | | | Stable | | | Stable | |
| $\mathcal{W}_s$ | 0.24 [0.63] | | | 5.17 [0.02] | | | 5.93 [0.01] | | | 4.75 [0.03] | | | 0.01 [0.92] | | | 3.38 [0.07] | |

*Note.* This table reports estimation results of the NARDL model specified in Equation (6), obtained using the one-step estimation approach of Shin et al. (2014). A general-to-specific procedure is used to arrive at the final NARDL model specification. Here, we set the maximum lag order equal to 12 and sequentially drop the insignificant dynamic regressors, with a 5% unidirectional decision rule. $\chi^2_{SC}$, $\chi^2_{HET}$, $\chi^2_{FF}$, and $\chi^2_{NOR}$ denote the LM tests for serial correlation (Breusch-Godfrey), heteroskedasticity (Breusch-Pagan), functional form (Ramsey's RESET), and normality (Jarque-Bera), respectively. Furthermore, CUSUM(SQ) denotes the test for stability of the regression coefficients and $\mathcal{W}_s$ is the Wald statistic for the test of short-run additive symmetry ($H_0 : \sum_{j=0}^{q-1} \pi_j^+ = \sum_{j=0}^{q-1} \pi_j^-$). Asymptotic $p$-values are reported in brackets for all tests. Lastly, in order to conserve space we do not present the coefficient estimates for the set of control variables.

# Appendix E Monte Carlo Simulation Two-Step NARDL

As discussed in Section 3.2, in our empirical study we employ the two-step approach of Cho et al. (2020) to estimate the NARDL model. Here, FM-OLS is used in the first step to estimate the long-run relationship, whereas the short-run dynamics are estimated by OLS in the second step. While Cho et al. (2020) present derivations and simulation results for the case of $k = 1$ and $k > 1$ asymmetric independent variables, our NARDL model includes both symmetric and asymmetric regressors. Therefore, slight alterations to the procedure of Cho et al. (2020) are required. Note that these changes do not affect the asymptotic theory associated with the two-step procedure. To demonstrate the validity of this approach, we further investigate the finite sample properties of the estimator and the Wald test statistics by means of simulation.

## E.1 Finite Sample Performance Two-Step Estimator

First, similar to Cho et al. (2020), we generate data according to the following data generating process (DGP):

$$\Delta y_t = c + \rho\varepsilon_{t-1} + \varphi\Delta y_{t-1} + \pi^+\Delta x_t^+ + \pi^-\Delta x_t^- + \pi\Delta z_t + e_t, \tag{E.1}$$

where $\varepsilon_{t-1} := y_{t-1} - \alpha - \beta^+ x_{t-1}^+ - \beta^- x_{t-1}^- - \beta z_{t-1}$, $\Delta w_t = \kappa\Delta w_{t-1} + \sqrt{1-\kappa^2}v_t$, $w_t = (x_t, z_t)'$, and $(e_t, v_t')' \sim$ i.i.d.$N(0_3, I_3)$. The parameter values are set to $(\alpha, \beta^+, \beta^-, \beta, c, \rho, \varphi, \pi^+, \pi^-, \pi, \kappa) = (0, 2, 1, 0.5, 0, -2/3, \varphi, 1, 0.5, 0.75, 0.5)$, where $\varphi$ and the sample size $T$ both take on a range of values as shown in the tables below.

In the two-step estimation approach, we specific the long-run and short-run relationships as

$$y_t = \alpha + \lambda x_t^+ + \eta x_t + \gamma z_t + \varepsilon_t \quad \text{and} \quad \Delta y_t = c + \rho\widehat{\varepsilon}_{t-1} + \varphi\Delta y_{t-1} + \pi^+\Delta x_t^+ + \pi^-\Delta x_t^- + \pi\Delta z_t + e_t,$$

where $\widehat{\varepsilon}_t := y_t - \widehat{\alpha} - \widehat{\lambda}x_t^+ - \widehat{\eta}x_t - \widehat{\gamma}z_t$. Here, we first obtain $\widehat{\alpha}$, $\widehat{\lambda}$, $\widehat{\eta}$, and $\widehat{\gamma}$ through FM-OLS, from which we derive $\widehat{\beta}^+$, $\widehat{\beta}^-$, and $\widehat{\beta}$. Conditional on $\widehat{\varepsilon}_t$, the short-run parameters are subsequently estimated by OLS. In total, the simulation exercise is performed $R = 10,000$ times, after which we compute the finite sample bias and mean squared error of the estimated parameters. The results are presented in Table E.1.

## E.2 Finite Sample Performance Wald Statistics

Next, we assess the empirical level properties and power of the Wald tests outlined in Section 3.2.3. Regarding the long run, we test the null $H_0 : \beta^+ - \beta^- = 0$ versus the alternative $H_1 : \beta^+ - \beta^- \neq 0$. We use the DGP specified in Equation (E.1) and the parameter values listed above, this time setting $\beta^+ = 1$ (for the levels) or $\beta^+ = 1.01$ (for the power). Note that the levels and power are determined by comparing the calculated test statistics to the critical values of the $\chi^2$-distribution with one degree of freedom at the 1%, 5%, and 10% significance levels. The results are presented in Table E.2.

Similarly, regarding the short run we test the null $H_0 : \pi^+ - \pi^- = 0$ versus the alternative $H_1 : \pi^+ - \pi^- \neq 0$. Again, we simulate data according to Equation (E.1) and use the parameter values reported in Section E.1. For the empirical levels we set $\pi^+ = 0.5$. The results are presented in Table E.3.

Table E.1: Finite Sample Performance Two-Step NARDL Estimation

| | | Bias | | | | | Mean Squared Error | | | | |
|---|---|---|---|---|---|---|---|---|---|---|---|
| | $T$ | 50 | 100 | 200 | 300 | 500 | 50 | 100 | 200 | 300 | 500 |
| $\varphi = -0.50$ | $\beta$ | −0.012 | 0.001 | 0.000 | −0.001 | 0.000 | 0.042 | 0.009 | 0.002 | 0.001 | 0.000 |
| | $\beta^+$ | −0.221 | −0.084 | −0.030 | −0.014 | −0.006 | 0.089 | 0.015 | 0.002 | 0.001 | 0.000 |
| | $\beta^-$ | −0.175 | −0.064 | −0.025 | −0.011 | −0.004 | 0.091 | 0.013 | 0.002 | 0.001 | 0.000 |
| | $\rho$ | −0.157 | −0.065 | −0.029 | −0.016 | −0.008 | 0.043 | 0.009 | 0.003 | 0.001 | 0.001 |
| | $\varphi$ | 0.106 | 0.045 | 0.019 | 0.011 | 0.006 | 0.018 | 0.005 | 0.001 | 0.001 | 0.000 |
| | $\pi$ | −0.018 | −0.005 | −0.002 | −0.002 | 0.000 | 0.051 | 0.017 | 0.006 | 0.004 | 0.002 |
| | $\pi^+$ | −0.039 | −0.013 | −0.004 | 0.000 | 0.001 | 0.145 | 0.054 | 0.023 | 0.014 | 0.008 |
| | $\pi^-$ | −0.084 | −0.027 | −0.018 | −0.009 | −0.005 | 0.164 | 0.056 | 0.023 | 0.014 | 0.008 |
| $\varphi = -0.25$ | $\beta$ | 0.010 | 0.004 | 0.001 | 0.001 | 0.000 | 0.030 | 0.006 | 0.001 | 0.000 | 0.000 |
| | $\beta^+$ | −0.153 | −0.056 | −0.017 | −0.007 | −0.003 | 0.054 | 0.009 | 0.001 | 0.000 | 0.000 |
| | $\beta^-$ | −0.121 | −0.045 | −0.014 | −0.006 | −0.002 | 0.062 | 0.009 | 0.001 | 0.000 | 0.000 |
| | $\rho$ | −0.136 | −0.059 | −0.026 | −0.015 | −0.008 | 0.036 | 0.010 | 0.003 | 0.002 | 0.001 |
| | $\varphi$ | 0.071 | 0.030 | 0.011 | 0.005 | 0.003 | 0.013 | 0.005 | 0.002 | 0.001 | 0.001 |
| | $\pi$ | −0.010 | −0.004 | −0.001 | −0.001 | 0.000 | 0.042 | 0.015 | 0.006 | 0.004 | 0.002 |
| | $\pi^+$ | −0.030 | −0.007 | −0.002 | −0.001 | 0.000 | 0.131 | 0.051 | 0.022 | 0.014 | 0.009 |
| | $\pi^-$ | −0.065 | −0.032 | −0.016 | −0.007 | −0.005 | 0.143 | 0.051 | 0.022 | 0.014 | 0.008 |
| $\varphi = 0.00$ | $\beta$ | 0.026 | 0.008 | 0.002 | 0.001 | 0.001 | 0.022 | 0.004 | 0.001 | 0.000 | 0.000 |
| | $\beta^+$ | −0.087 | −0.032 | −0.008 | −0.004 | −0.001 | 0.034 | 0.005 | 0.001 | 0.000 | 0.000 |
| | $\beta^-$ | −0.080 | −0.028 | −0.007 | −0.004 | −0.001 | 0.042 | 0.006 | 0.001 | 0.000 | 0.000 |
| | $\rho$ | −0.124 | −0.055 | −0.026 | −0.016 | −0.010 | 0.032 | 0.009 | 0.004 | 0.002 | 0.001 |
| | $\varphi$ | 0.035 | 0.013 | 0.005 | 0.003 | 0.001 | 0.009 | 0.004 | 0.002 | 0.001 | 0.001 |
| | $\pi$ | −0.003 | −0.002 | 0.000 | 0.001 | 0.000 | 0.038 | 0.014 | 0.006 | 0.004 | 0.002 |
| | $\pi^+$ | −0.017 | −0.007 | −0.003 | −0.003 | 0.000 | 0.125 | 0.048 | 0.021 | 0.014 | 0.008 |
| | $\pi^-$ | −0.049 | −0.023 | −0.012 | −0.010 | −0.005 | 0.129 | 0.049 | 0.021 | 0.014 | 0.008 |
| $\varphi = 0.25$ | $\beta$ | 0.027 | 0.011 | 0.002 | 0.002 | 0.000 | 0.019 | 0.004 | 0.001 | 0.000 | 0.000 |
| | $\beta^+$ | −0.029 | −0.015 | −0.004 | −0.004 | −0.002 | 0.026 | 0.004 | 0.001 | 0.000 | 0.000 |
| | $\beta^-$ | −0.051 | −0.022 | −0.005 | −0.004 | −0.002 | 0.047 | 0.006 | 0.001 | 0.000 | 0.000 |
| | $\rho$ | −0.096 | −0.045 | −0.022 | −0.014 | −0.009 | 0.023 | 0.008 | 0.003 | 0.002 | 0.001 |
| | $\varphi$ | 0.007 | 0.005 | 0.002 | 0.002 | 0.000 | 0.008 | 0.004 | 0.002 | 0.001 | 0.001 |
| | $\pi$ | −0.007 | −0.001 | 0.002 | 0.001 | 0.001 | 0.034 | 0.013 | 0.006 | 0.004 | 0.002 |
| | $\pi^+$ | −0.017 | −0.012 | −0.006 | −0.007 | −0.002 | 0.121 | 0.049 | 0.022 | 0.015 | 0.008 |
| | $\pi^-$ | −0.036 | −0.021 | −0.009 | −0.008 | −0.004 | 0.127 | 0.049 | 0.021 | 0.014 | 0.008 |
| $\varphi = 0.50$ | $\beta$ | 0.023 | 0.004 | −0.002 | 0.002 | 0.000 | 0.025 | 0.004 | 0.001 | 0.000 | 0.000 |
| | $\beta^+$ | 0.023 | −0.014 | −0.008 | −0.008 | −0.005 | 0.035 | 0.005 | 0.001 | 0.000 | 0.000 |
| | $\beta^-$ | −0.041 | −0.035 | −0.013 | −0.010 | −0.006 | 0.078 | 0.009 | 0.001 | 0.000 | 0.000 |
| | $\rho$ | −0.057 | −0.024 | −0.012 | −0.008 | −0.005 | 0.012 | 0.004 | 0.002 | 0.001 | 0.001 |
| | $\varphi$ | −0.011 | 0.002 | 0.001 | 0.002 | 0.001 | 0.006 | 0.003 | 0.001 | 0.001 | 0.000 |
| | $\pi$ | −0.008 | −0.005 | −0.003 | 0.000 | 0.001 | 0.036 | 0.014 | 0.006 | 0.004 | 0.002 |
| | $\pi^+$ | −0.002 | −0.016 | −0.011 | −0.007 | −0.005 | 0.122 | 0.050 | 0.022 | 0.014 | 0.008 |
| | $\pi^-$ | −0.041 | −0.024 | −0.010 | −0.007 | −0.004 | 0.129 | 0.048 | 0.022 | 0.014 | 0.008 |

*Note.* This table reports the finite sample bias and mean squared error of the two-step NARDL estimation approach, using FM-OLS in the first step and OLS in the second step. Here, we vary the degree of autocorrelation $\varphi$ and sample size $T$. The data are generated according to the following process: $\Delta y_t = -(2/3)u_{t-1} + \varphi\Delta y_{t-1} + \Delta x_t^+ + 0.5\Delta x_t^- + 0.75\Delta z_t + e_t$, where $u_t := y_t - 2x_t^+ - x_t^- - 0.5z_t$, $\Delta w_t = 0.5\Delta w_{t-1} + \sqrt{1-0.5^2}v_t$, $w_t = (x_t, z_t)'$, and $(e_t, v_t')' \sim$ i.i.d.$N(0_3, I_3)$. Results are obtained using $R = 10,000$ replications.

Table E.2: Finite Sample Performance Wald Test for Long-Run Symmetry

| | $T$ | 50 | 100 | 200 | 300 | 500 | 1,000 | 2,500 | 5,000 |
|---|---|---|---|---|---|---|---|---|---|
| *Panel A: Levels* | | | | | | | | | |
| $\varphi = -0.50$ | 1% | 18.14 | 14.46 | 8.90 | 5.68 | 3.48 | 2.28 | 1.62 | 1.32 |
| | 5% | 30.70 | 26.42 | 18.72 | 14.66 | 10.76 | 8.22 | 6.76 | 6.06 |
| | 10% | 38.92 | 34.92 | 26.32 | 21.68 | 17.56 | 15.16 | 12.62 | 11.90 |
| $\varphi = -0.25$ | 1% | 15.12 | 9.90 | 6.08 | 4.90 | 3.78 | 3.08 | 1.82 | 1.78 |
| | 5% | 26.68 | 21.12 | 15.08 | 12.30 | 11.04 | 9.34 | 7.52 | 6.84 |
| | 10% | 34.70 | 29.56 | 21.86 | 19.14 | 18.36 | 15.70 | 13.78 | 12.64 |
| $\varphi = 0.00$ | 1% | 10.72 | 6.94 | 4.24 | 3.28 | 3.14 | 2.10 | 1.66 | 1.36 |
| | 5% | 21.86 | 16.36 | 11.84 | 11.12 | 9.16 | 7.54 | 6.60 | 6.60 |
| | 10% | 29.62 | 23.60 | 18.94 | 18.40 | 15.58 | 13.70 | 12.68 | 12.00 |
| $\varphi = 0.25$ | 1% | 8.14 | 4.86 | 2.50 | 2.40 | 1.80 | 1.48 | 1.26 | 1.14 |
| | 5% | 17.36 | 13.00 | 8.36 | 7.64 | 7.12 | 6.08 | 5.54 | 5.28 |
| | 10% | 24.56 | 19.18 | 14.16 | 13.30 | 12.98 | 11.82 | 10.62 | 10.14 |
| $\varphi = 0.50$ | 1% | 5.04 | 2.72 | 0.70 | 0.72 | 0.78 | 0.50 | 0.56 | 0.54 |
| | 5% | 12.56 | 8.48 | 4.04 | 4.34 | 3.66 | 3.28 | 3.50 | 3.34 |
| | 10% | 19.26 | 14.12 | 8.56 | 9.24 | 7.80 | 7.00 | 7.52 | 7.14 |
| *Panel B: Power* | | | | | | | | | |
| $\varphi = -0.50$ | 1% | 18.74 | 14.82 | 20.10 | 38.50 | 81.98 | 99.78 | 100.00 | 100.00 |
| | 5% | 30.88 | 26.22 | 33.88 | 53.66 | 89.12 | 99.94 | 100.00 | 100.00 |
| | 10% | 38.98 | 34.18 | 42.74 | 61.80 | 91.42 | 99.94 | 100.00 | 100.00 |
| $\varphi = -0.25$ | 1% | 17.14 | 12.78 | 20.22 | 45.44 | 84.84 | 99.86 | 100.00 | 100.00 |
| | 5% | 28.86 | 23.62 | 34.36 | 59.82 | 91.40 | 99.96 | 100.00 | 100.00 |
| | 10% | 37.94 | 31.44 | 43.16 | 67.24 | 93.88 | 99.96 | 100.00 | 100.00 |
| $\varphi = 0.00$ | 1% | 11.70 | 10.26 | 19.34 | 44.50 | 85.04 | 99.88 | 100.00 | 100.00 |
| | 5% | 23.14 | 21.18 | 33.80 | 60.50 | 91.70 | 99.96 | 100.00 | 100.00 |
| | 10% | 30.56 | 28.82 | 43.24 | 69.02 | 94.28 | 100.00 | 100.00 | 100.00 |
| $\varphi = 0.25$ | 1% | 8.64 | 7.52 | 15.26 | 40.86 | 83.94 | 99.86 | 100.00 | 100.00 |
| | 5% | 18.54 | 16.80 | 29.74 | 58.44 | 91.72 | 99.96 | 100.00 | 100.00 |
| | 10% | 25.62 | 24.18 | 39.76 | 67.42 | 94.56 | 99.98 | 100.00 | 100.00 |
| $\varphi = 0.50$ | 1% | 5.28 | 3.40 | 6.78 | 28.34 | 76.78 | 99.68 | 100.00 | 100.00 |
| | 5% | 13.32 | 11.20 | 19.40 | 49.22 | 88.72 | 99.98 | 100.00 | 100.00 |
| | 10% | 21.14 | 17.96 | 29.64 | 60.54 | 92.50 | 99.98 | 100.00 | 100.00 |

*Note.* This table reports the empirical levels and power (in percentages) of the Wald test statistic for symmetry of the long-run parameters, testing the null $H_0 : \beta^+ - \beta^- = 0$ versus the alternative $H_1 : \beta^+ - \beta^- \neq 0$. We employ the two-step NARDL estimation approach, using FM-OLS in the first step and OLS in the second step. Here, we vary the degree of autocorrelation $\varphi$ and sample size $T$. The data are generated according to the following process: $\Delta y_t = -(2/3)u_{t-1} + \varphi \Delta y_{t-1} + \Delta x_t^+ + 0.5\Delta x_t^- + 0.75\Delta z_t + e_t$, where $u_t := y_t - x_t^+ - x_t^- - 0.5z_t$ (Panel A), $u_t := y_t - 1.01x_t^+ - x_t^- - 0.5z_t$ (Panel B), $\Delta w_t = 0.5\Delta w_{t-1} + \sqrt{1 - 0.5^2} v_t$, $w_t = (x_t, z_t)'$, and $(e_t, v_t')' \sim$ i.i.d.$N(0_3, I_3)$. Results are obtained using $R = 10,000$ replications.

Table E.3: Finite Sample Performance Wald Test for Short-Run Symmetry

| | $T$ | 50 | 100 | 200 | 300 | 500 | 1,000 | 2,500 | 5,000 |
|---|---|---|---|---|---|---|---|---|---|
| *Panel A: Levels* | | | | | | | | | |
| $\varphi = -0.50$ | 1% | 4.50 | 2.38 | 1.50 | 1.18 | 1.26 | 1.04 | 1.36 | 1.18 |
| | 5% | 11.78 | 8.02 | 6.00 | 6.42 | 5.64 | 5.18 | 5.80 | 4.90 |
| | 10% | 18.28 | 14.44 | 11.42 | 11.66 | 10.84 | 9.98 | 10.72 | 9.94 |
| $\varphi = -0.25$ | 1% | 4.16 | 2.30 | 1.66 | 1.04 | 1.24 | 0.92 | 1.12 | 0.82 |
| | 5% | 11.32 | 7.74 | 6.40 | 5.70 | 5.20 | 5.32 | 5.62 | 5.08 |
| | 10% | 17.32 | 13.76 | 11.78 | 11.00 | 9.82 | 10.30 | 10.12 | 10.04 |
| $\varphi = 0.00$ | 1% | 4.42 | 2.36 | 1.22 | 1.28 | 1.88 | 1.16 | 1.20 | 1.14 |
| | 5% | 11.58 | 8.10 | 5.60 | 5.54 | 6.14 | 5.20 | 4.94 | 4.98 |
| | 10% | 17.32 | 13.30 | 10.92 | 10.84 | 11.46 | 9.40 | 10.00 | 10.12 |
| $\varphi = 0.25$ | 1% | 3.64 | 2.26 | 1.42 | 1.48 | 1.00 | 1.14 | 1.04 | 1.14 |
| | 5% | 10.36 | 7.40 | 5.94 | 6.12 | 4.50 | 4.96 | 4.84 | 5.42 |
| | 10% | 17.30 | 12.58 | 11.52 | 11.36 | 9.18 | 10.98 | 9.54 | 10.34 |
| $\varphi = 0.50$ | 1% | 3.86 | 2.12 | 1.42 | 1.30 | 1.36 | 0.94 | 1.08 | 0.96 |
| | 5% | 10.38 | 6.96 | 6.26 | 5.92 | 5.98 | 5.10 | 5.20 | 5.48 |
| | 10% | 16.84 | 12.82 | 11.40 | 10.90 | 11.02 | 9.82 | 10.08 | 10.90 |
| *Panel B: Power* | | | | | | | | | |
| $\varphi = -0.50$ | 1% | 12.26 | 19.76 | 36.90 | 52.88 | 79.22 | 98.46 | 100.00 | 100.00 |
| | 5% | 24.90 | 36.90 | 59.42 | 73.96 | 92.06 | 99.72 | 100.00 | 100.00 |
| | 10% | 33.88 | 47.62 | 69.88 | 82.76 | 95.50 | 99.90 | 100.00 | 100.00 |
| $\varphi = -0.25$ | 1% | 12.14 | 17.94 | 36.60 | 52.58 | 78.70 | 98.44 | 100.00 | 100.00 |
| | 5% | 24.86 | 34.50 | 59.40 | 74.64 | 91.80 | 99.72 | 100.00 | 100.00 |
| | 10% | 33.84 | 45.70 | 70.68 | 83.98 | 95.66 | 99.88 | 100.00 | 100.00 |
| $\varphi = 0.00$ | 1% | 12.28 | 18.56 | 36.28 | 51.60 | 78.82 | 98.42 | 100.00 | 100.00 |
| | 5% | 26.02 | 36.08 | 59.12 | 73.36 | 91.56 | 99.78 | 100.00 | 100.00 |
| | 10% | 35.54 | 46.68 | 70.10 | 82.48 | 95.18 | 99.96 | 100.00 | 100.00 |
| $\varphi = 0.25$ | 1% | 11.56 | 18.52 | 34.42 | 52.28 | 77.74 | 98.16 | 100.00 | 100.00 |
| | 5% | 25.06 | 35.80 | 56.96 | 74.06 | 91.58 | 99.70 | 100.00 | 100.00 |
| | 10% | 34.16 | 46.62 | 68.46 | 82.46 | 95.30 | 99.90 | 100.00 | 100.00 |
| $\varphi = 0.50$ | 1% | 11.08 | 18.14 | 34.50 | 48.66 | 77.32 | 98.40 | 100.00 | 100.00 |
| | 5% | 24.08 | 34.60 | 56.44 | 71.98 | 91.06 | 99.84 | 100.00 | 100.00 |
| | 10% | 33.36 | 45.80 | 67.88 | 81.56 | 95.28 | 99.98 | 100.00 | 100.00 |

*Note.* This table reports the empirical levels and power (in percentages) of the Wald test statistic for symmetry of the short-run parameters, testing the null $H_0 : \pi^+ - \pi^- = 0$ versus the alternative $H_1 : \pi^+ - \pi^- \neq 0$. We employ the two-step NARDL estimation approach, using FM-OLS in the first step and OLS in the second step. Here, we vary the degree of autocorrelation $\varphi$ and sample size $T$. The data are generated according to the following process: $\Delta y_t = -(2/3)u_{t-1} + \varphi \Delta y_{t-1} + 0.5\Delta x_t^+ + 0.5\Delta x_t^- + 0.75\Delta z_t + e_t$ (Panel A), $\Delta y_t = -(2/3)u_{t-1} + \varphi \Delta y_{t-1} + \Delta x_t^+ + 0.5\Delta x_t^- + 0.75\Delta z_t + e_t$ (Panel B), $u_t := y_t - 2x_t^+ - x_t^- - 0.5z_t$, $\Delta w_t = 0.5\Delta w_{t-1} + \sqrt{1 - 0.5^2} v_t$, $w_t = (x_t, z_t)'$, and $(e_t, v_t')' \sim$ i.i.d.$N(0_3, I_3)$. Results are obtained using $R = 10,000$ replications.